SKB

TECHNICAL REPORT 86-11

Hydraulic fracturing rock stress measurements in borehole Gi-1 Gideå study site, Sweden

Bjarni Bjarnason and Ove Stephansson

Division of Rock Mechanics,
Luleå University of Technology, Sweden

April 1986

SVENSK KÄRNBRÄNSLEHANTERING AB
SWEDISH NUCLEAR FUEL AND WASTE MANAGEMENT CO

BOX 5864 S-102 48 STOCKHOLM
TEL 08-665 28 00 TELEX 13108-SKB

HYDRAULIC FRACTURING ROCK STRESS MEASUREMENTS IN BOREHOLE Gi-1, GIDEÅ STUDY SITE, SWEDEN

Bjarni Bjarnason and Ove Stephansson
Division of Rock Mechanics,
Luleå University of Technology, Sweden

April 1986

CONTENTS

LIST OF SYMBOLS AND ABBREVIATIONS

C_1 : First conventional pressurization cycle

C_2 : Second conventional pressurization cycle etc.

P_c : Confining pressure

P_{c1} : First breakdown pressure

P_{c2} : Second breakdown pressure etc.

P_i : Internal pressure for laboratory specimens

P_{ic} : Critical internal pressure

P_o : Pore pressure

P_p : Packer pressure

P_s : Shut in pressure

P_{s1} : First shut-in pressure

P_{s2} : Second shut-in pressure etc.

Q : Flow rate

T : Tensile strength

T_f : Tensile strength measured in the field

T_{lab}: Laboratory tensile strength

T_{app}: Applied tensile strength

σ_h : Minimum horizontal stress

σ_H : Maximum horizontal stress

σ_{HI} : Maximum horizontal stress from the first breakdown method

σ_{HII}: Maximum horizontal stress from the second breakdown method

σ_t : Tangential stress

σ_v : Theoretical vertical stress

σ_z : Axial stress

SUMMARY

This report presents the results from rock stress measurements conducted by the hydraulic fracturing method at Gideå in Northern Sweden. The Gideå area is one of the sites selected for extensive investigation within the Swedish programme for final disposal of radioactive waste in deep seated repositories in crystalline rock. The measurements were conducted in a vertical borehole within one of the repository blocks in the area. Successful measurements were conducted at 25 test sections, from the ground surface down to a maximum depth of 500 m. The results show moderate rock stresses and no extreme values are recorded. The minimum horizontal stress, σ_h, increases with depth at a rate close to that of the theoretical vertical stress, σ_v, representing a stress field close to isotropic in the vertical plane containing σ_h and σ_v. At depth around 300 m there is a change in the gradient of the minimum horizontal stress.

The maximum horizontal stress, σ_H, is determined according to the second breakdown method, applying tensile strength values from the field measurements. The maximum stress is low at surface but increases at a higher rate than the minimum horizontal stress, maintaining a nearly constant ratio of 1.6 to the minimum horizontal stress at all depths. The average orientation of the maximum horizontal stress, determined from hydrofracture orientations, is N67^{0}E.

1 INTRODUCTION

1.1 General

By Swedish law, the responsibility of safe final storage of spent nuclear fuel is laid upon the owners of the nuclear reactors operating in the country. SKB, The Swedish Nuclear Fuel and Waste Management Company, commonly established and owned by the reactor companies, has the role of developing a safe method of final disposal of all radioactive waste. The investigation presented in this report was ordered by SKB and carried out by the Division of Rock Mechanics at the Luleå University of Technology, Sweden.

1.2 Scope of the investigation

The programme of final disposal of high-level radioactive waste in Sweden has concentrated on the concept of deep seated repositories in crystalline bedrock. Within this programme, a number of study sites has been selected for extensive surface and borehole investigations to obtain a better knowledge of the geological, hydrogeological and geochemical conditions at large depths. Gideå, one of these study sites, is situated near the coast in northern Sweden, about 30 km NE of Örnsköldsvik (Figure 1).

One of the important factors governing the overall safety of a repository at 500 m depth in the bedrock is that of rock stresses in the repository area. A knowledge ot the virgin stress field is important in three main aspects:

- The hydraulic conductivity of the rock will partly depend upon the natural stress field.

- The detailed design of orientation, shape and size of the excavations will partly depend on magnitudes and orientations of the principal stresses.

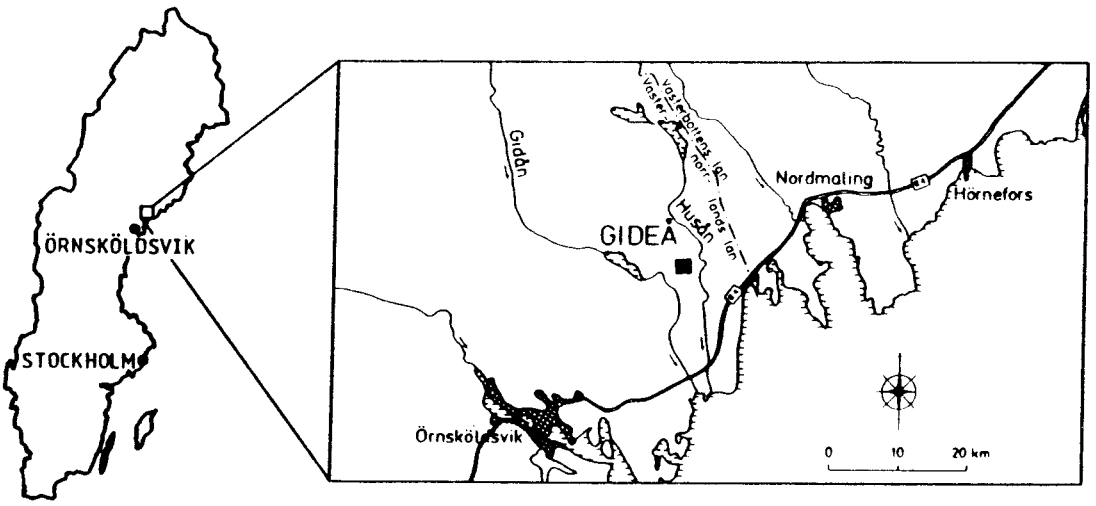

Figure 1. Geographical location of the Gideå study site.

- The mechanical stability of the rock mass will mainly depend on the stress situation in the area.

Thus, the virgin rock stresses will be one of the key factors in the final selection of repository site.

The present investigation was conducted to assess the virgin rock stresses within the study site at Gideå. The horizontal stress field was measured at 31 test points to a depth of 500 m in a vertical borehole in one of the two repository blocks in the area. Measurements were conducted by the hydraulic fracturing stress measuring method.

2 BASIC THEORY OF THE HYDROFRACTURING METHOD

2.1 Theoretical background

The calculation of stresses from hydrofracturing measurements, first proposed by Hubbert and Willis (1957), is based on a simple analytical solution of stresses around a circular opening in an infinite plate. The rock is assumed to be isotropic, linear elastic and impermeable. The solution is two-dimensional, only considering stresses in a plane perpendicular to the borehole axis. Thus, when measuring stresses in vertical boreholes, one of the principal stresses (σ_v) is assumed to be vertical, parallel to the axis of the borehole, and equal to the overburden pressure.

$$\sigma_v = \gamma D \qquad (1)$$

where γ is the unit weight of the rock and D is the depth to the measuring point.

The tangential stress in a point at distance r from the center of the borehole is given by equation (2), Figure 2:

$$\sigma_t = \frac{\sigma_H + \sigma_h}{2}\left(1 + \frac{a^2}{r^2}\right) - \frac{\sigma_H - \sigma_h}{2}\left(1 + 3\frac{a^4}{r^4}\right)\cos 2\theta \qquad (2)$$

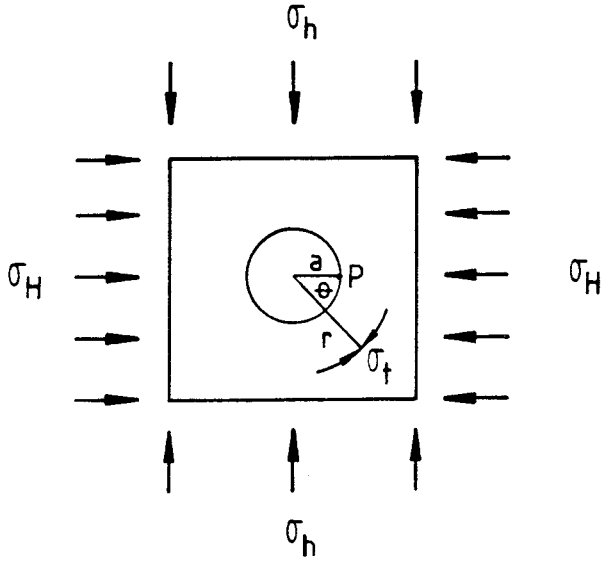

Figure 2. Stresses in a plane perpendicular to a vertical borehole.

Since the rock material is assumed to be isotropic, the hydrofracture will initiate in the borehole wall at point P, in a plane perpendicular to the minimum horizontal stress, σ_h. The value of the minimum horizontal stress is taken to be equal to the instantaneous shut-in pressure, P_s, obtained when the hydraulic pressure in the fracture is in equilibrium with the stresses acting across the fracture plane, i.e.

$$\sigma_h = P_s \tag{3}$$

At point P (Figure 2), $r = a$ and $\Theta = 0$, and from equation (2) we get the tangential stress, σ_t, at the borehole wall as

$$\sigma_t = 3\sigma_h - \sigma_H \tag{4}$$

where σ_H is the maximum horizontal stress.

To create a fracture in an intact rock wall, both the tangential stress at the borehole wall, σ_t, and the tensile strength of the rock, T, must be exceeded. Thus we must have the following critical hydraulic pressure in the borehole, P_{c1}, to create a fracture:

$$P_{c1} = 3\sigma_h - \sigma_H + T \tag{5}$$

from which

$$\sigma_H = 3\sigma_h + T - P_{c1} \tag{6}$$

If the rock is porous, the reduction in critical hydraulic pressure for fracture initiation, due to the pore pressure in the rock, is given by

$$P_{c1} = 3\sigma_h - \sigma_H + T - P_o \tag{7}$$

The necessity for an independent determination of the tensile strength of the rock can be eliminated by using the second critical pressure, P_{c2}, obtained from the second pressurization

$$T_f = P_{c1} - P_{c2} \tag{8}$$

where T_f is the field tensile strength. Inserting $T = T_f$ in equation (6) gives

$$\sigma_H = 3\sigma_h - P_{c2} \tag{9}$$

Equations (1), (3) and (9) and the orientation of the hydrofracture determine the complete stress state at the test depth, under the assumption that one of the principal stresses is vertical and equal to the overburden pressure.

2.2 Hydrofracturing data analysis

2.2.1 Vertical stress, σ_v

The vertical stress is calculated from equation (1), where the unit weight of the rock, γ, is taken to be 27 kN/m^3, and the depth is expressed in meters.

2.2.2 Minimum horizontal stress, σ_h

When the water flow to the pressurized section is shut down the hydrofracture is open and propagating, and the water pressure is higher than the rock stresses acting perpendicular to the fracture plane. Immediately after shut down the pressure generally drops steeply to a stable value, called the instantaneous shut-in pressure, P_s, (Figure 3). P_s corresponds to the pressure when the fracture closes, preventing further flow into the formation. Thus the pressure at the time of closing, equals the rock stresses acting across the fracture plane. If we assume that the fracture initiates and propagates perpendicular

to the direction of σ_h we obtain according to equation (3), $\sigma_h = P_s$. In ideal cases the instantaneous shut-in pressure is indicated by a sharp break in the pressure time curve. In practice, however, the shut-in pressure often bleeds off slowly after the fracture has closed, and P_s cannot be readily defined. A number of methods have been proposed for the identification of P_s. A short review of conventional methods is given by Ångman (1984) and Stephansson and Ångman (1986). None of the methods can be regarded as being appropriate in all cases.

The selection of the appropriate method in each case depends on the general characteristics of the pressure-time curves. The curves from Gideå generally show a sudden pressure drop following shut down, and a nearly linear bleed off after fracture closure. The instantaneous shut-in pressures, P_{s1}, P_{s2}, etc. are defined by the intersection of the tangents to the post peak portions of the curves shown in Figure 3.

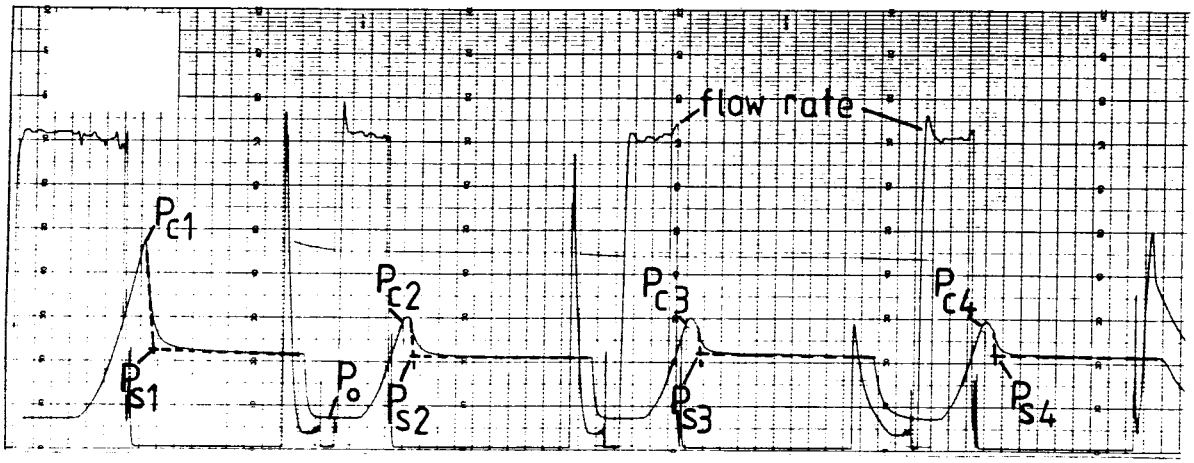

Figure 3. A typical pressure-time record from the hydrofracturing measurements in Gideå, (Gi-1, 345 m depth).

It is a common experience in hydrofracturing work that the instantaneous shut-in pressure tends to decrease somewhat in repeated pressurization cycles, as the fracture propagates away from the hole. P_s usually stabilizes after two or three cycles, Zoback and Haimson (1982). The shut-in pressure most representative of σ_h is the final value, Hickman and Zoback (1982). The shut-in pressures selected to represent σ_h in Gideå, are usually the values from the third pressurization cycle.

2.2.3 Maximum horizontal stress, σ_H

The maximum horizontal stress has been calculated by two methods; a) the first breakdown method (equation (6)) and b) the second breakdown method (equation (9)). The first method uses the first breakdown pressure, P_{c1} and a tensile strength derived from laboratory tests on rock cores for calculating σ_H. The second method uses the second breakdown pressure, P_{c2}, assuming that the tensile strength of the rock is the difference between first and second breakdown pressures, $P_{c1} - P_{c2}$.

The second breakdown pressure, P_{c2}, is defined as the pressure at which the initial borehole pressurization rate in the later cycles deviates from that established in the first cycle, prior to breakdown, Figure 4.

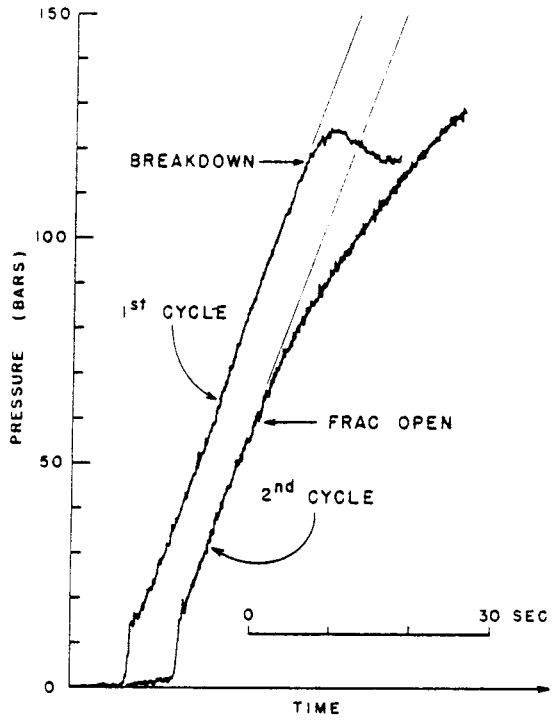

Figure 4. Method of identifying the second breakdown pressure, P_{c2}. (After Hickman and Zoback 1983).

2.2.4 Tensile strength of the rock

The laboratory tensile strength is determined as follows:

A core specimen with planar and parallel ends, and a central hole, is subjected to confining pressure in a bi-axial cell and loaded axially in a small press, Figure 5. The central hole is pressurized by oil or water until fracturing occurs. Sealings in the hole ("packers") confine the internal pressure to the central portion of the rock core. This simulates actual field conditions, although on a much smaller scale. Acoustic emission during fracturing is recorded to detect the fracture initiation. Specimens are tested at variable confining pressures, always keeping the axial load slightly higher than the confinement. The results from the individual tests are shown in Table A3 in the Appendix.

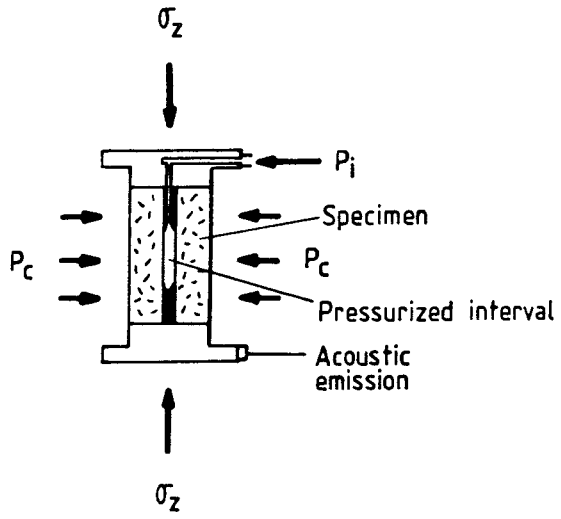

Figure 5. Laboratory simulation of hydraulic fracturing for determination of the tensile strength.

The critical internal pressure, P_{ic}, is plotted against the confining pressure for each test series, Figure 6, and the laboratory tensile strength is defined as the intercept on the y-axis at zero confining pressure.

The central hole in the laboratory specimens is 10 mm in diameter whereas the borehole for stress measurements in the field is 56 mm in diameter. The appropriate method of extrapolation of data from the small scale laboratory tests, to the field borehole remains an open question. Here we use a deterministic fracture mechanics approach based on Paris and Sih (1965) and applied by Doe et al. (1983) for the evaluation of tensile strength data for hydrofracturing stress measurements. The hydrofracture is assumed to initiate on the largest grain boundaries in the intact rock. The ratio of the tensile strength for two borehole diameters is inversely proportional to the stress intensity coefficient for the two diameters. Applying stress intensity coefficients from Paris and Sih (1965) we get the results shown in Table 1 for intact rock in the Gideå borehole.

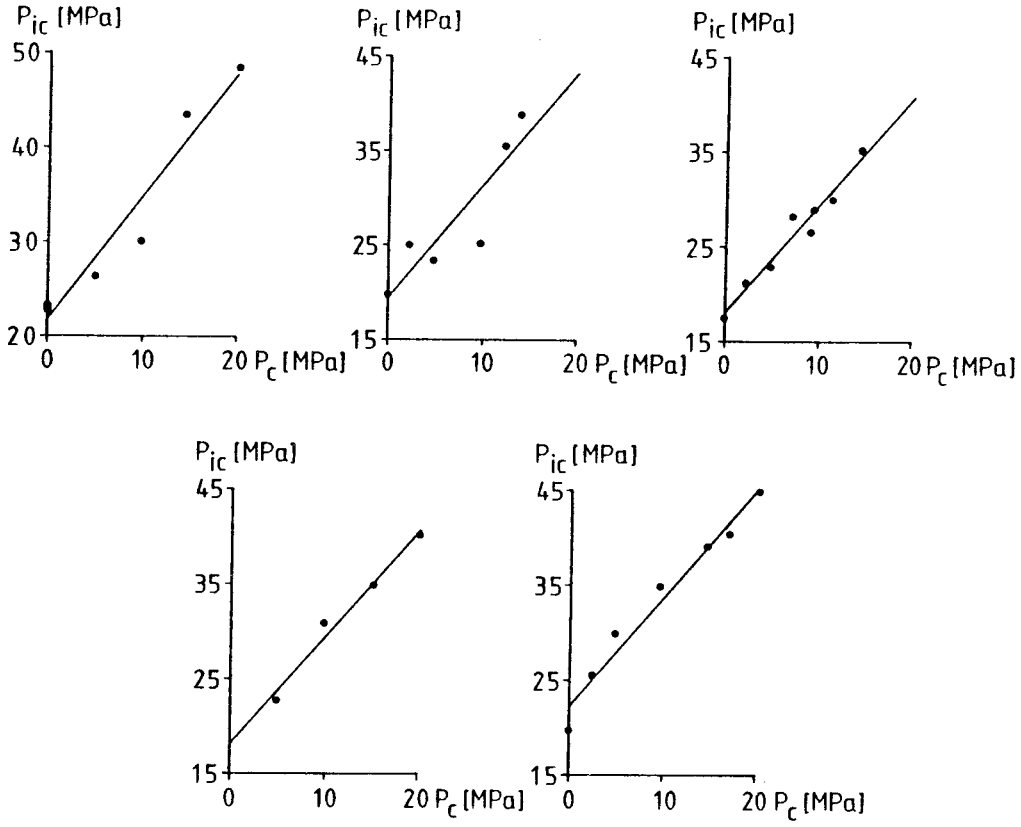

Figure 6. Results from laboratory testing of tensile strength.

Table 1. Tensile strength for different borehole diameters from deterministic fracture mechanics analysis.

Depth (m)	Grain size (mm)	T_{lab} (10 mm) (MPa)	T_{app} (56 mm) (MPa)
50	2	12.6	8.8
150	5	19.4	12.0
250	5	17.9	11.1
380	5	18.3	11.3
460	5	22.3	13.8

Mean T_{app} 11.4 MPa

2.2.5 Pore pressure, P_o

The pore pressure term in equation (7) is a matter of controversy within hydraulic fracturing studies. Some authors, e.g. Haimson (1978) and Doe et al. (1983) include the pore pressure when crystalline rocks are considered. Others, e.g. Rummel et al.(1982) neglect the pore pressure, and state that the subtraction of the water column from the maximum horizontal stress in impermeable, crystalline rocks will give misleading and meaningless results. In this study the pore pressure at depth is neglected in the evaluation of the virgin rock stresses.

2.2.6 Direction of σ_H

In the cases where two long and vertical hydrofractures have been detected, the mean direction (strike) of the two fractures is taken to be the direction of σ_H at the test point.

3 HYDROFRACTURING APPARATUS AND TESTING PROCEDURE

3.1 Field instrumentation

From a functional point of view, the field equipment can be divided into the following systems:

- Multihose, drum and feeder
- Packers
- Pump and water control system
- Orientation instrument
- Data recording system

The multihose is 500 m long, composed of 3 high-pressure hoses; 8, 8 and 10 mm inner diameter, a 16 wire signal cable, and a wire to carry the load in the hole. A cross section of the hose is shown in Figure 7. The hose is wound on a hydraulically driven drum. It is run up and down the hole by the drum and a hydraulic feeder placed directly above the hole.

During tests, the packers are pressurized through one of the 8 mm hoses, while water to the test section runs through the 10 mm hose. The third high pressure hose acts as a reserve hose.

Two packer systems are used during the measurements:

- A straddle packer system during fracturing and shut-in registration
- An impression packer for fracture orientation

The straddle packer is composed of two high pressure packers, separated by the 65 cm long test section. The impression packer is a single packer covered by soft impression rubber, Figure 8. Both packer systems are supplied with a special pressure-release valve, to release the remaining pressure from the packers after depressurizing the packer

line at surface. All packer elements are made of inexpensive, nylon reinforced rubber hoses, with pressed-on steel bindings. The active sealing length of the packers is about 1 m. Maximum differential pressure for the packers is 35-40 MPa.

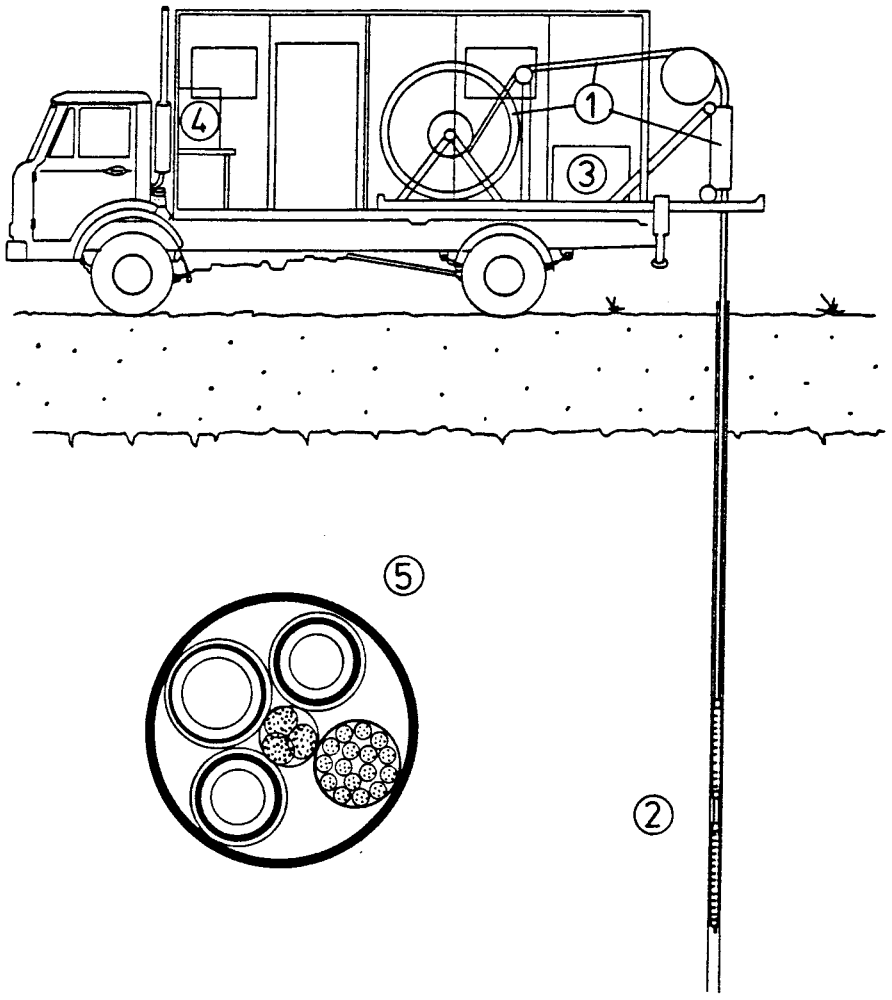

Figure 7. Field instruments; 1) multihose, drum and feeder, 2) packers, 3) pump and water control system, 4) recording unit, 5) cross section of the multihose.

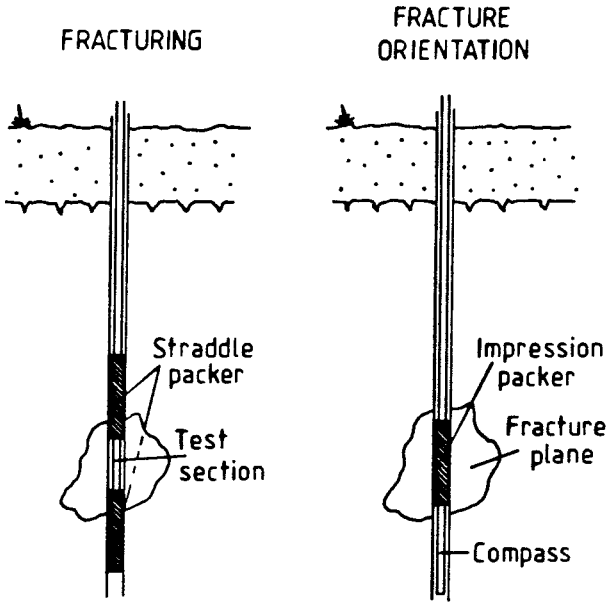

Figure 8. Test configuration in the borehole.

High pressure water is supplied by a hydraulically driven 3 cylinder piston pump. The maximum flow rate is 15 l/min and the maximum pressure is 100 MPa. The pressure in the system is set to a predetermined constant value for each test by two bypass valves. The packer pressure and the test section pressure are controlled independently. The water is supplied by a 900 l tank and all return water is returned to the tank so that water consumption is minimized, Figure 9.

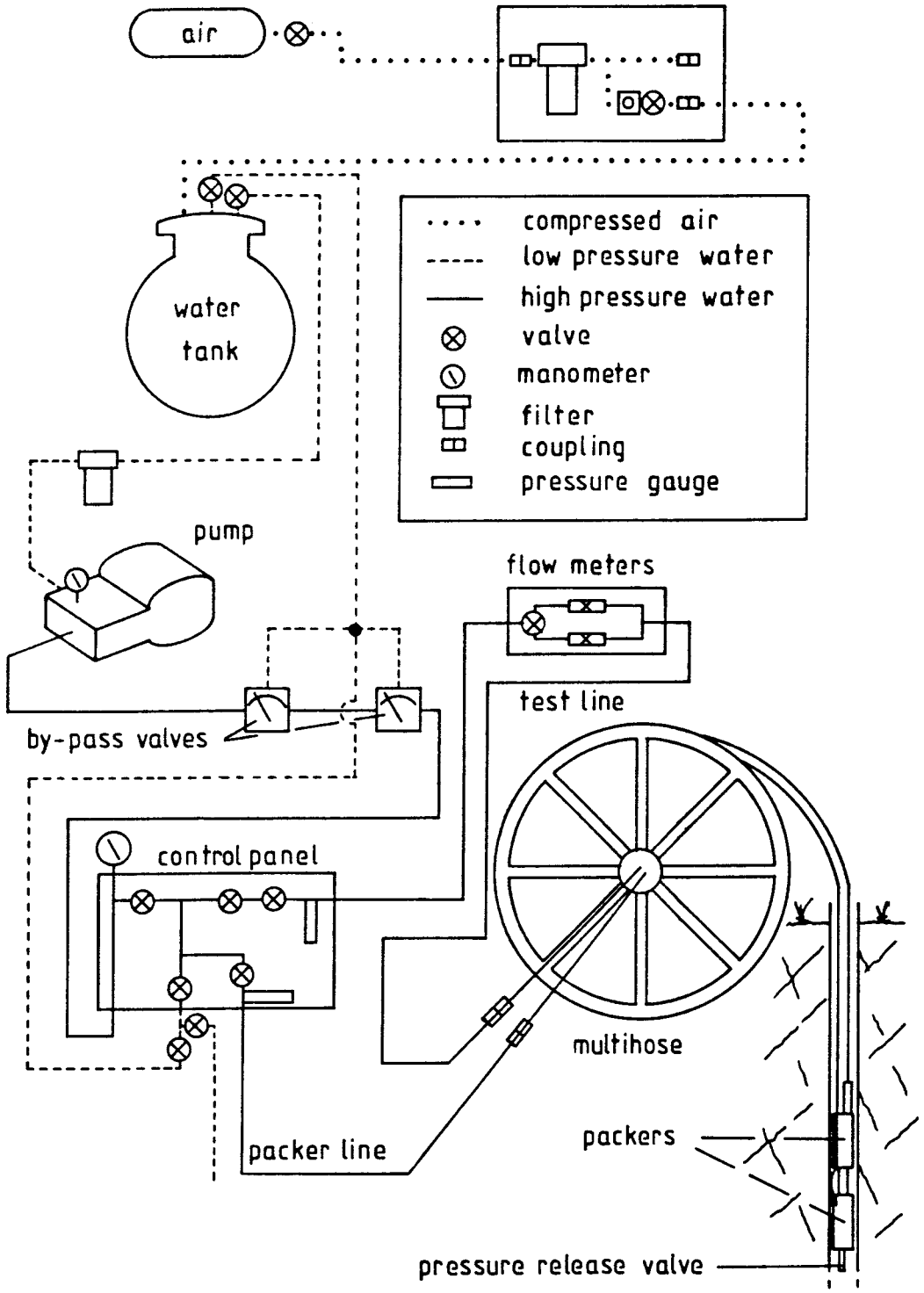

Figure 9. Pump and water control system.

Orientation instrument;

Packer orientation during impression was recorded by a single-shot magnetic compass attached to the lower end of the packer. The photographic film from the compass camera shows inclination and direction of the borehole and the orientation of the packer referred to magnetic north. The compass is fixed in a stainless steel barrel 3 m below the packer end.

Data recording system;

The following parameters were recorded during testing:

- Downhole pressure in the test section, measured immediately above the straddle packer.
- Test section pressure measured at surface.
- Packer pressure measured at surface.
- Water flow rate to test section.

All four parameters were continuously recorded on a time based strip chart recorder.

3.2 Test procedure

The drillcore is examined for the selection of test sections free of fractures. A straddle packer is then lowered to the desired depth, and inflated hydraulically with water, Figure 8. The sealed-off interval between the packers is pressurized simultaneously, maintaining a higher pressure in the packers, but a low, constant pressure difference between the packers and the fracturing interval. The fluid pressure acting on the borehole wall in the sealed off section will ultimately exceed the combined support by the tangential stresses and the tensile strength of the rock. A fracture will then initiate in the

borehole wall. This is indicated by a sudden drop in the recorded pressure, Figure 3. The pressure in the test section is recorded for some minutes after shut-down of the pressure line. The pressure in the test section is then released after which, 2-3 additional pressurization cycles are conducted. When the test is completed, the inflatable packers are depressurized and the assembly is moved to the next interval to be tested.

After all fracturing tests in the hole are terminated, a preliminary evaluation of test results is performed. Based on the evaluation, impressions are taken at the test sections that give the most reliable results. The impression packer is lowered to the precise depth of the hydrofracturing section and hydraulically pressurized for 20-30 minutes. Careful inspection of the packer will define the trace of the hydrofracture as well as any other openings or joints. The orientation of the impression packer, found by a magnetic compass during the impression period, enables the determination of the hydrofracture orientation.

The two steps, pressurization and fracture orientation, complete the hydrofracturing test and enable the determination of both the magnitudes and the orientations of the principal stresses in the plane perpendicular to the axis of the borehole.

4 SITE CONDITIONS

4.1 Geology

The information in this section is mainly derived from SKBF/KBS (1983) and Ahlbom et al. (1983).

The actual study site lies within a more than 100 km^2 plateau about 100 m above sea level. It consists of a smaller elevated area with rather flat topography. The ground level within the site ranges between 80 and 130 m above sea level.

The main rock type within the site is veined migmatized gneiss. The rock is characterized by veins and other irregular bodies of varying mineralogical composition. The veins generally strike NE, usually dipping shallowly, 10-30^0, to the north. Pegmatites also occur within the site in the form of small bodies and metre-wide dikes. Diabase occurs as narrow (1-10m), steep dikes striking E-W.

The Gideå site is surrounded by regional fracture zones striking WNW and NW. These zones lie outside the area studied in detail and coincide largely with the valleys of the Gideå and Husån rivers, located about 5 km apart.

At the study site the rock is cut by a number of local fracture zones. These are smaller in width and extension than the regional zones. Figure 10 shows the location of the local fracture zones at the surface. The local zones bound a triangular block with a surface area of 1.8 km^2. This block is intersected by two narrow fracture zones, about 4 m wide. The zone numbers in Figure 10 refer to information in Table 2.

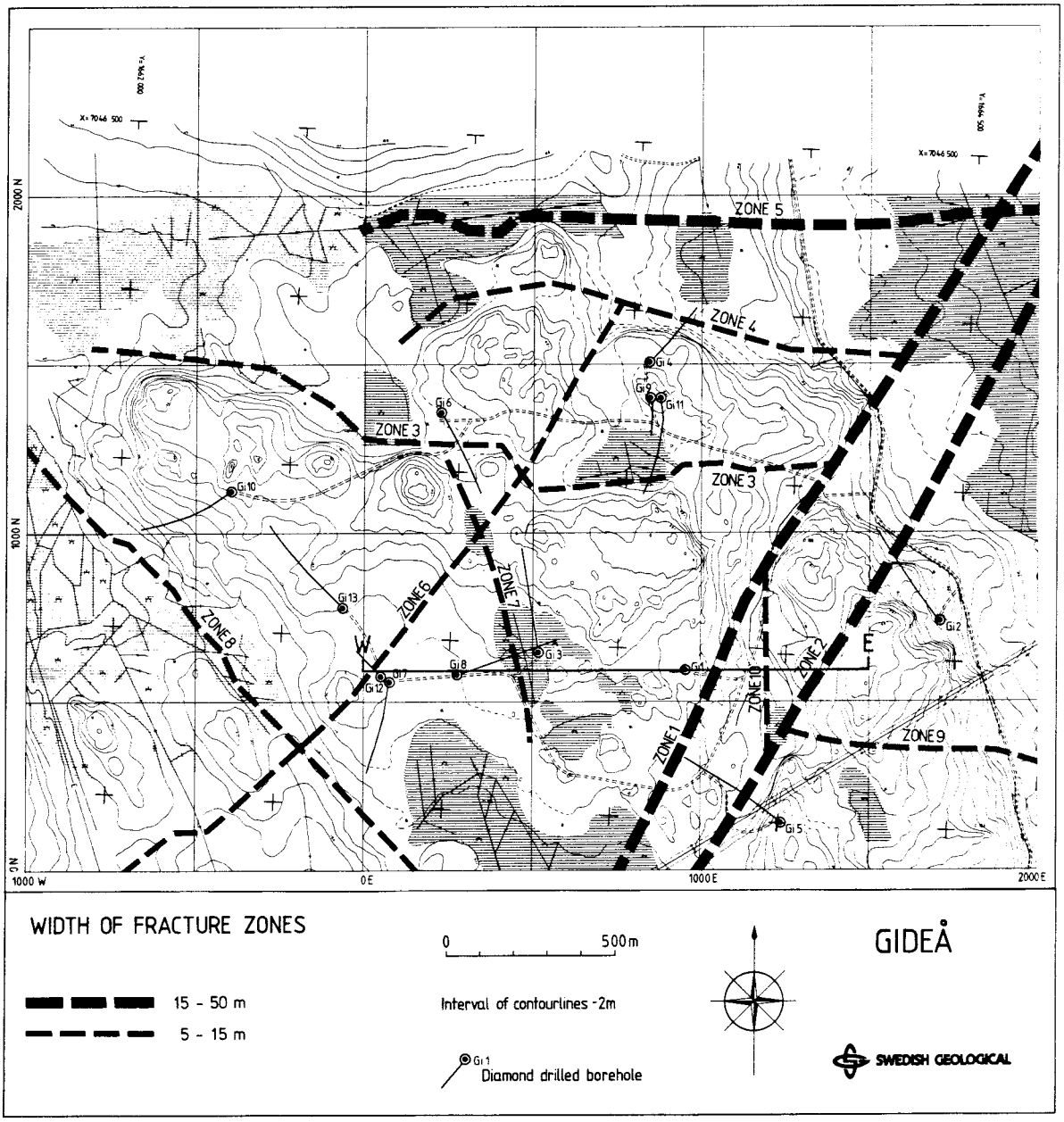

Figure 10. Fracture zones at surface within the study site at Gideå. (After Ahlbom et al. 1983).

Table 2. Summary of fracture zones within the study site.

Fracture zone	Dip (degrees)	True width (m)
1	40 SE	23
2	70 NW	11
3A	30 N	17
3B	80 N	6
4	90	10
5	80 N *	50 *
6	70 SE	4
7	75 E	4
8	70 SW *	10 *
9	70 N *	5 *
10	90 *	5 *

* Calculated from geophysical information

The local fracture zones have been identified and studied in detail by means of air photo interpretation, geophysical measurements at surface and by percussion and core drilling. Altogether 13 deep coreholes (218-701 m deep) and 24 percussion boreholes have been drilled within the study site. The location and direction of each corehole is shown in Figure 10.

The stress measurements were conducted in hole Gi-1, the only vertical corhole in the area. The location of Gi-1 with respect to the fracture zones is shown in a vertical section from E to W in Figure 11. The horizontal location of the hole and the section line is marked on Figure 10. The borehole lies close to fracture zone no. 1 at surface but at depth it is centrally located in the repository block.

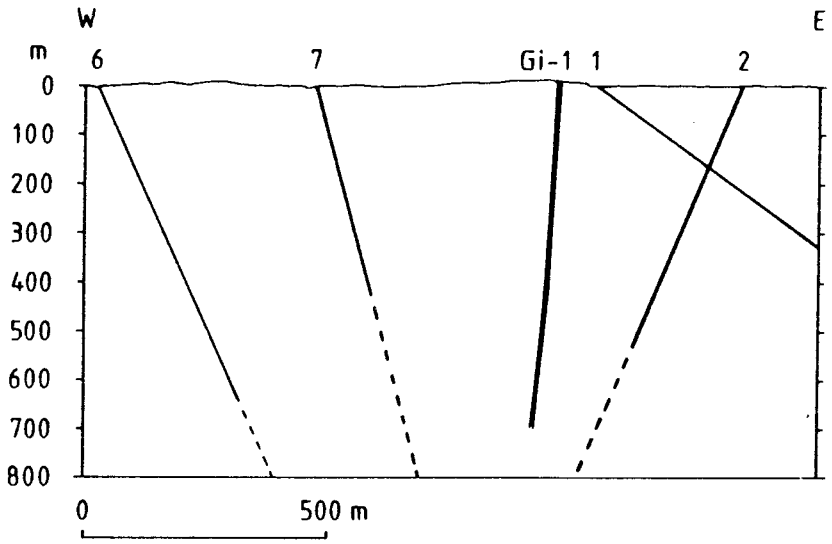

Figure 11. A vertical E-W section showing the location of borehole Gi-1 with respect to the nearest fracture zones.

Fracturing of the rock mass (excluding the fracture zones) has been mapped on outcrops and in the drillcore. The variation in fracture frequency with depth is shown in Figure 12. A fracture log and a hydraulic conductivity log from borehole Gi-1 are presented in Figure 13.

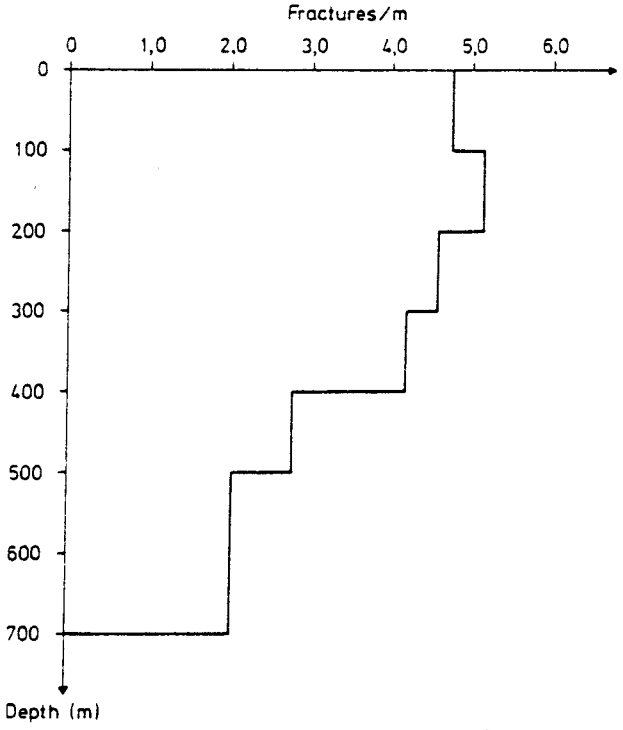

Figure 12. Fracture frequency in the rock mass at Gideå. (After Ahlbom et al. 1983).

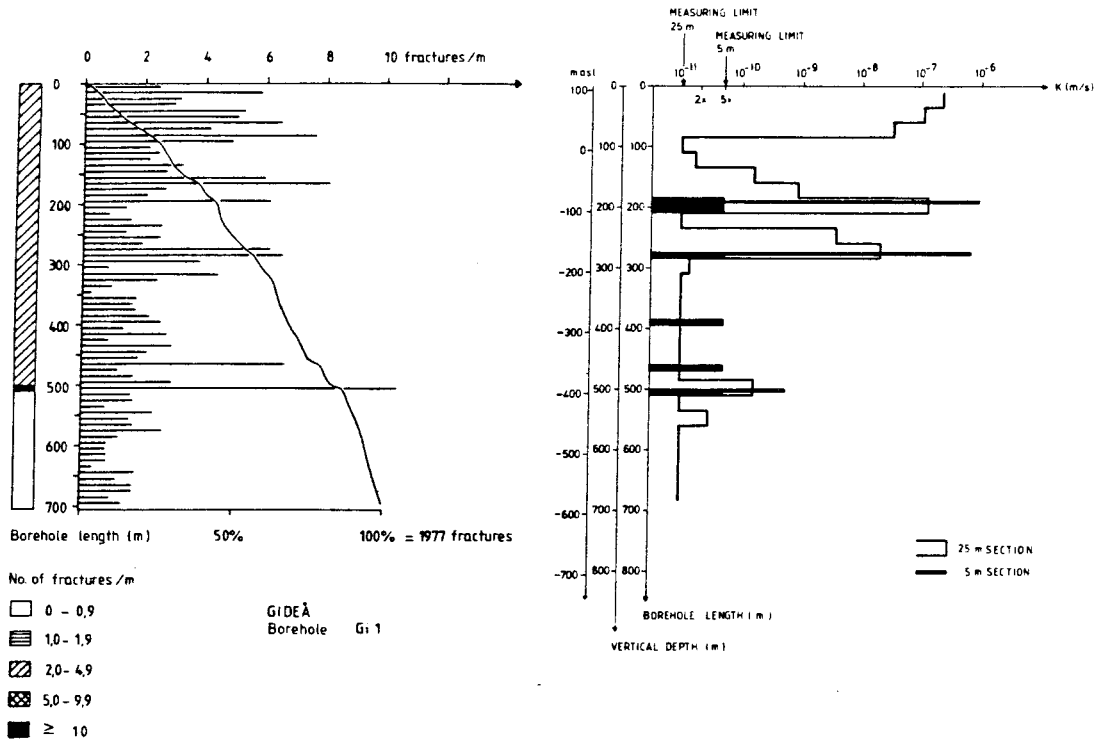

Figure 13. A fracture frequency log for 10 m sections and a hydraulic conductivity log for Gi-1. (After Ahlbom et al. 1983).

4.2 Mechanical properties of the rock

A study of the intrinsic mechanical properties of granitic rocks from Gideå has been conducted at the Division of Rock Mechanics at the Luleå University of Technology. The results are presented by Ljunggren et al. (1985). The following tests were conducted:

- Sound velocity measurements for determination of:

  Dynamic elastic modulus (E_d), dynamic Poisson's ratio (ν_d), bulk modulus (B_d), primary and shear wave velocities and the intensity of microfracturing.

- Uniaxial compression test for the determination of:

  Static elastic modulus (E_s), static Poisson's ratio (ν_s), uniaxial compressive strength (σ_c) and brittleness.

- Brazilian test for tensile strength determination (indirect).

- Triaxial test for the determination of:

  Modulus of elasticity (E) and compressive strength (σ_c).

- Three point bending test for the determination of:

  Fracture toughness (K_{Ic}), elastic modulus (E_b) and energy release rate (G).

Alltogether, 12 rock samples were tested with each method. Six samples out of these were of migmatitic gneiss and the remaining six were of migmatitic granite. All samples were collected from the drill core of borehole Gi-1.

The values of only few selected parameters are presented here. In general, the results from the study were quite average compared to other granitic rocks. The modulus of elasticity varied between 50 - 65 GPa for both rock types and the Poisson's ratio between 0.08 - 0.33, depending on the method applied. The mean values of uniaxial compressive strengths and the Brazilian tensile strength were as follows:

	Uniaxial compression strength σ_c (MPa)	Brazilian tensile strength (MPa)
Migmatitic gneiss	128	18.1
Migmatitic granite	201	12.3

The uniaxial compression strength for migmatitic gneiss is rather low while its tensile strength is comparatively high. The tensile strength results for individual samples are shown in Figure 14.

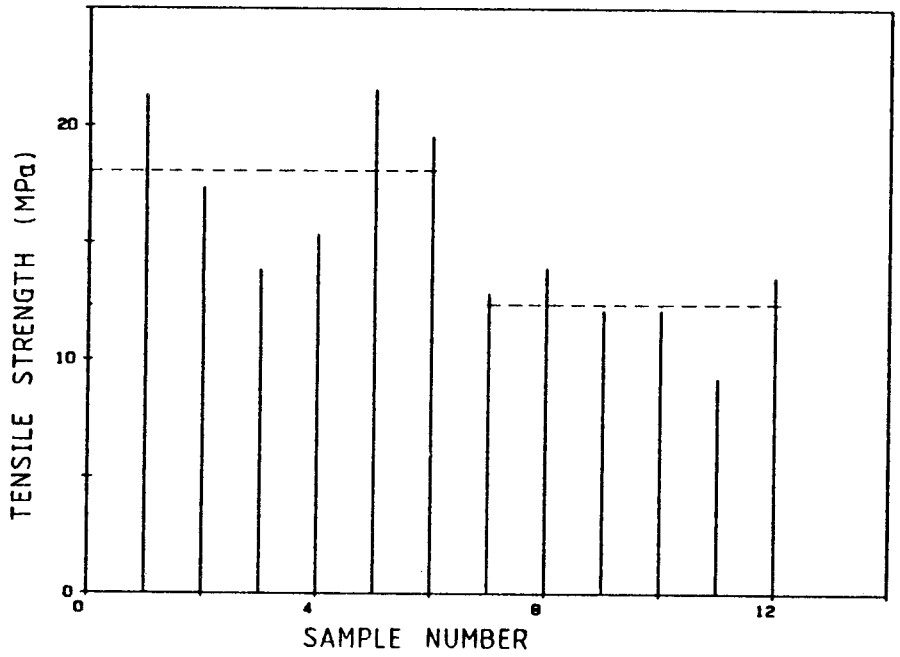

Figure 14. Brazilian test results from borehole Gi-1.
Samples 1-6 : migmatitic gneiss
Samples 1-12: migmatitic granite
Dotted lines show average values.

5 EXPERIMENTAL RESULTS AND STRESS STATE VERIFICATION

5.1 Experimental results

Rock stresses were measured at 31 points from 14.5 m depth down to 501 m. Fracture impressions were attempted at all 31 points. Six of the impressions showed single, horizontal or subhorizontal fractures in the test section. The results from those six points are rejected in the evaluation of the state of stress.

The compiled pressure data from the remaining 25 measuring points are shown in Table A1 in the Appendix. The pressure-time records from most of the test sections are reproduced in the Appendix. Due to faint colours of the original curves, some of these were not suitable for photographic reproduction. Calculated rock stresses are presented in Table 3 in this chapter. The maximum horizontal stress is calculated according to the first and the second breakdown methods. The field tensile strength, T_f, and the ratios between the maximum and the minimum horizontal stresses for both evaluation methods are also presented in Table 3. The results from the fracture impression work are shown in Table A2 in the Appendix. In Figure 15 the calculated stresses are plotted as a function of depth.

Table 3. Calculated rock stresses, Gi-1.

				First breakdown method		Second breakdown method		
	Field tensile strength	Vertical stress	Min horiz. stress	Max horiz. stress	Horiz. stress ratio	Max horiz. stress	Horiz. stress ratio	Stress difference
Depth (m)	T_f (MPa)	σ_v (MPa)	σ_h (MPa)	σ_{HI} (MPa)	$\frac{\sigma_{HI}}{\sigma_h}$	σ_{HII} (MPa)	$\frac{\sigma_{HII}}{\sigma_h}$	$\sigma_{HI}-\sigma_{HII}$ (MPa)
14.5	6.7	0.4	2.2	8.6	3.9	3.9	1.8	4.7
47.0	10.2	1.3	1.8	4.8	2.7	3.6	2.0	1.2
51.0	10.9	1.4	2.1	3.1	1.5	2.6	1.2	0.5
79.5	3.0	2.1	3.4	13.3	3.9	4.9	1.4	8.4
111.0	10.3	3.0	4.4	9.2	2.1	8.1	1.8	1.1
122.5	11.0	3.3	5.2	7.9	1.5	7.5	1.4	0.4
140.0	7.8	3.8	6.6	13.9	2.1	10.3	1.6	3.6
173.0	6.7	4.7	5.3	13.8	2.6	9.1	1.7	4.7
183.0	9.9	4.9	8.1	11.2	1.4	9.7	1.2	1.5
204.0	6.8	5.5	7.2	12.9	1.8	8.3	1.2	4.6
222.0	11.8	6.0	7.4	11.3	1.5	11.7	1.6	-0.4
273.0	10.2	7.4	8.8	16.4	1.9	15.2	1.7	1.2
325.0	7.7	8.8	8.8	16.1	1.8	12.4	1.4	3.7
345.0	9.3	9.3	11.1	20.9	1.9	18.8	1.7	2.1
400.9	10.9	10.8	11.4	21.9	1.9	21.4	1.9	0.5
402.0	14.7	10.9	10.9	15.9	1.5	19.2	1.8	-3.3
426.0	10.6	11.5	9.9	16.6	1.7	15.8	1.6	0.8
453.0	8.0	12.2	10.1	16.1	1.6	12.7	1.3	3.4
470.0	11.7	12.7	11.7	19.6	1.7	19.9	1.7	-0.3
481.5	6.5	13.0	12.6	25.6	2.0	20.7	1.6	4.9
483.0	11.5	13.0	12.1	19.2	1.6	19.3	1.6	-0.1
489.0	11.4	13.2	12.0	21.7	1.8	21.7	1.8	0
495.0	10.9	13.4	11.0	18.9	1.7	18.4	1.7	0.5
500.0	5.5	13.5	10.3	21.7	2.1	15.8	1.5	5.9
501.0	6.8	13.5	10.0	24.5	2.4	19.9	2.0	4.6

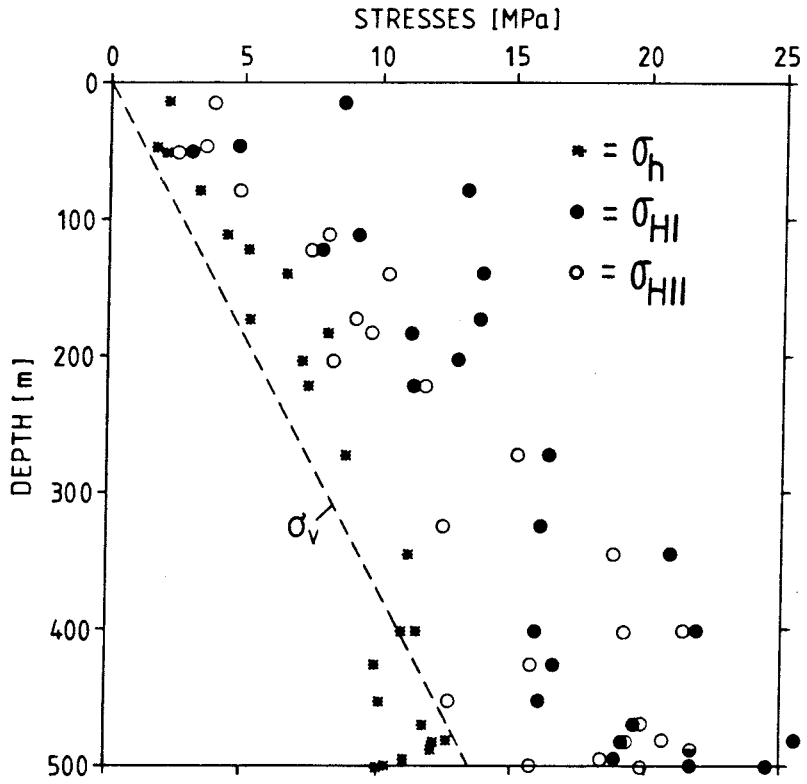

Figure 15. Calculated rock stresses as a function of depth in Gi-1.

5.2 Stress magnitudes

The minimum horizontal stress, σ_h is around 2 MPa close to the surface. Down to approximately 300 m depth it increases steadily at a rate close to that of the theoretical vertical stress, σ_v, Figure 15. In this interval σ_h is the intermediate principal stress, typically about 2 MPa higher than σ_v. At depths exceeding 300 m the minimum horizontal stress continues to increase but at a lower rate. Below an approximate depth of 400 m σ_h becomes smaller than σ_v, thus representing the minimum principal stress in the depth interval from 400-500 m. As the difference between the magnitudes of σ_h and σ_v is generally small the stress situation can be described as close to isotropic in the vertical plane containing σ_h and σ_v.

Compared to other hydrofracturing stress measurements in Sweden (Stephansson and Ångman (1984), Bjarnason et al.(1986)) the minimum horizontal stress at Gideå shows a very regular increase with depth and small scatter in magnitudes.

For the maximum horizontal stress the situation is not as clear:

Evaluation according to the first breakdown method results in a large scatter of the maximum horizonatal stress, σ_{HI}. The scatter is most pronounced near the surface. Thus, we obtain values of 3.1 MPa and 13.3 MPa at two neighbouring points at 51 m and 79.5 m depths respectively. The scatter is somewhat less at greater depths. The ratio between σ_{HI} and σ_h is plotted as a function of depth in Figure 16. The highest values, 3.9, are found near the surface. The ratio decreases and stabilizes with depth, generally lying just under 2 below 300 m depth.

The values of maximum horizontal stress from the second breakdown method, σ_{HII} give somewhat lower values than σ_{HI}. The scatter for the σ_{HII} data is smaller at the surface but increases with depth. The ratio of σ_{HII}/σ_h is fairly stable throughout the entire measuring depth (Figure 16), having a nearly constant value around 1.6.

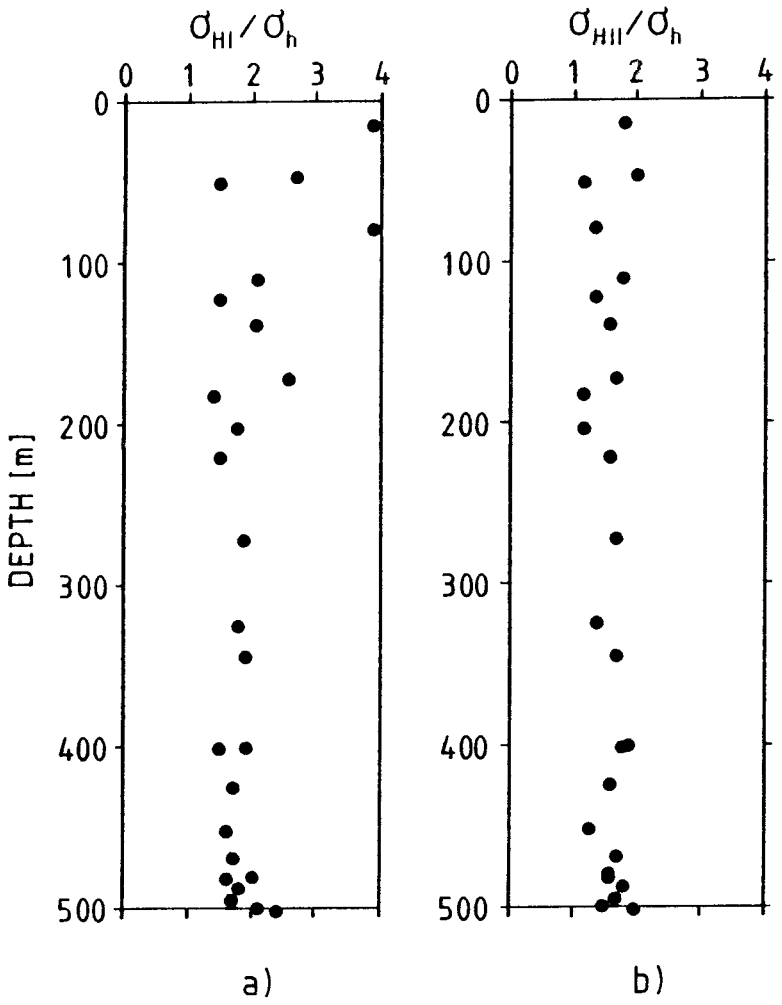

Figure 16. The ratio of maximum to minimum horizontal stresses a) σ_{HI}/σ_h versus depth, b) σ_{HII}/σ_h versus depth.

5.3 Interpretation of stress magnitudes versus depth.

In Figure 17 the horizontal stresses have been analyzed by means of linear regression analysis. All 25 points are included. The dotted curves are the 95 % confidence limits for the position of the regression lines.

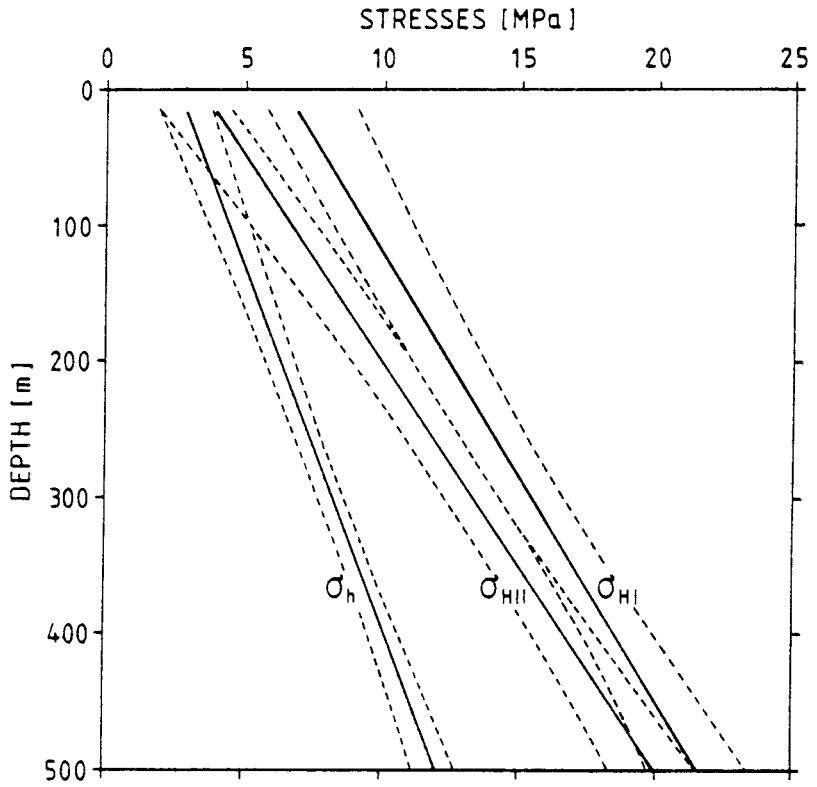

Figure 17. The variation in horizontal stress magnitudes with depth, according to linear regression analysis of all measuring points. The dotted curves are the 95 % confidence limits for the position of the regression lines.

As mentioned in section 5.2 the gradient for the minimum horizontal stress appears to change at depths around 300 m. Based on this observation, the σ_h values have been analysed by two separate regression lines, assuming a bend in the σ_h gradient around 300 m depth. The first regression fit involves the recordings from 14.5 m down to 273 m depth, the second involves points from 325 m down to the deepest measurement at 501 m. The results from the two different plots; the linear and the bi-linear, are presented in Figure 18. The regression line for the minimum horizontal stress, σ_h in Figure 18 a) intersects the trend of the σ_h values at an approximate depth of 150 m and again just below 400 m depth.

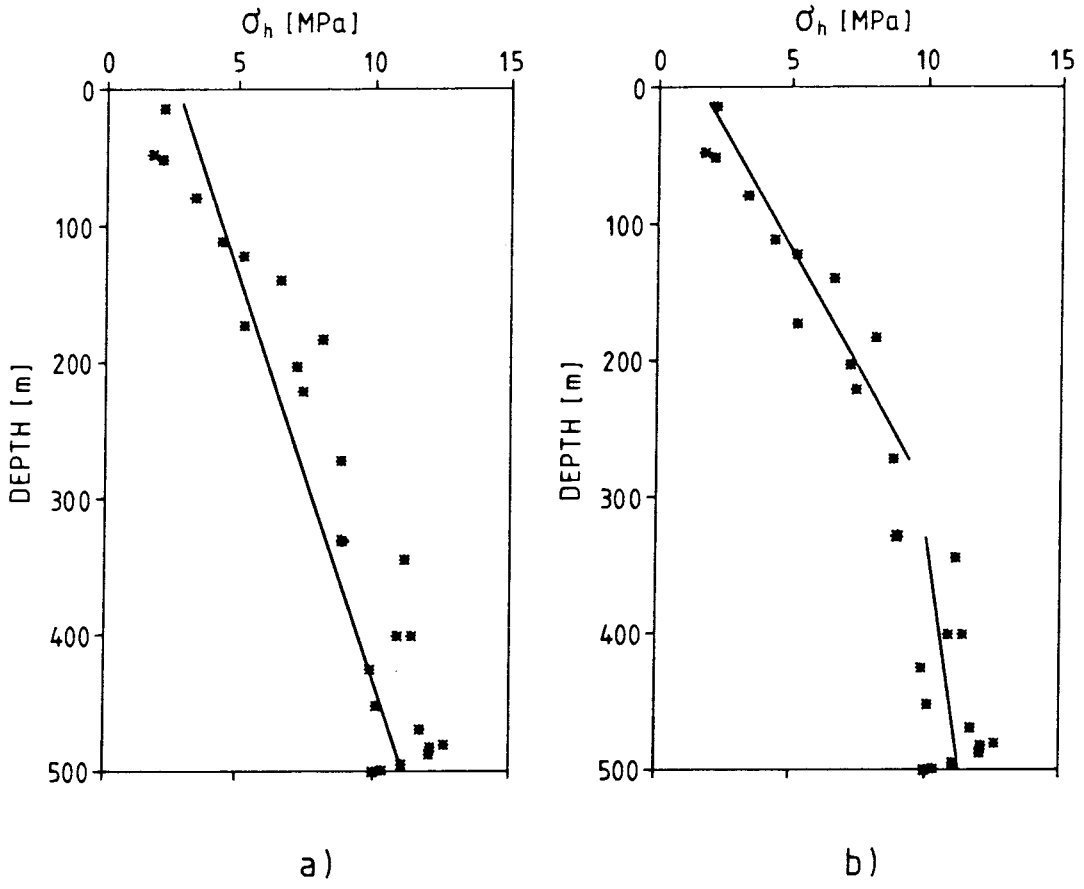

Figure 18. Linear regression analysis of the minimum horizontal stress as a function of depth assuming;
a) linear increase of σ_h throughout the measuring range
b) bend in the σ_h gradient around 300 m depth.

Figure 18 argues definitely in favour of the discontinuity approach.

In search for an explanation for the observed change in gradient of σ_h around 300 m depth we recall Figures 12 and 13:

Figure 12 shows fracture frequency as a function of depth for 100 m intervals in the rock mass within the Gideå site. Between 300 and 400 m depth the fracture frequency falls from about 4.7 to 2.7 fractures per metre.

Figure 13 shows the fracture frequency for 10 m sections and the hydraulic conductivity for borehole Gi-1. From 270 to 300 m depth the fracture frequency increases abruptly and again from 310 to 320 m

depth. From 320 m down to 500 m the fracture frequency is generally low with one exception around 460 m. The difference in fracture frequencies above and below 320 m depth in the borehole is also clear from the change in inclination of the cumulative curve at 320 m depth. The hydraulic conductivity data give the same picture. Around 280 m depth there is a sudden increase in the conductivity and the overall picture shows a significant decrease in K values below 300 m depth.

Thus, the change in the σ_h gradient around 300 m depth, observed in Figure 15 and further demonstrated in Figure 18 is reflected by the fracture characteristics of the rock mass in the area and especially by the decrease in fracture frequency below 300 m in borehole Gi-1.

Based on these observations, we assume the horizontal in-situ stress field, in the block penetrated by borehole Gi-1, to be characterized by a discontinuity in horizontal stress gradients at an approximate depth of 300 m. The results are presented in Figure 19.

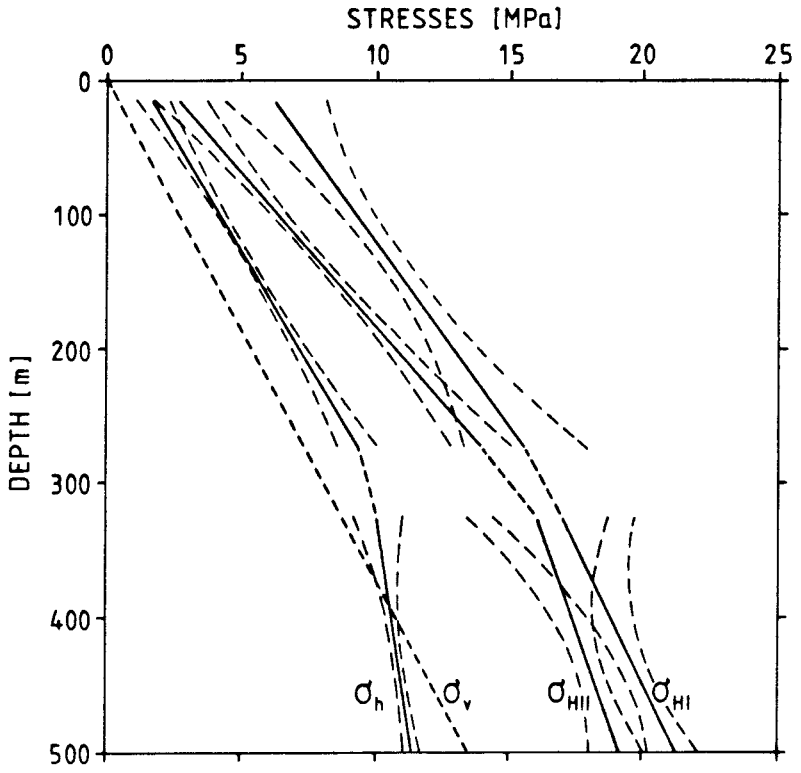

Figure 19. Linear regression analysis of the horizontal stresses at Gideå, according to the assumption of a bi-linear stress gradient. The dotted curves are 95 % confidence limits for the regression lines.

The upper regression lines end at 273 m depth and the lower ones begin at 325 m. In Figure 19 each pair of lines has been connected by a straight dotted line. The 95 % confidence limits have been calculated for each regression line. This results in broad confidence limits around 300 m depth. Furthermore, the number of observations behind each line is lower than in Figure 17, resulting in increased curvature of the confidence limits. However, at the central portion of each regression line in Figure 19 the confidence limits are tighter than those we obtain in Figure 17.

Figure 19 shows the difference in results between the first breakdown and the second breakdown methods. The σ_{HII} values are lower than the σ_{HI} values at all depths. The relative difference is highest at low stresses near the surface where σ_{HI} is about two times higher than σ_{HII}. The absolute difference between the two methods changes little with depth but the relative difference decreases considerably, being around 10 % at 500 m depth.

In Figure 20 the horizontal stress ratios, σ_{HI}/σ_h and σ_{HII}/σ_h have been plotted according to the assumption of bi-linear stress gradients.

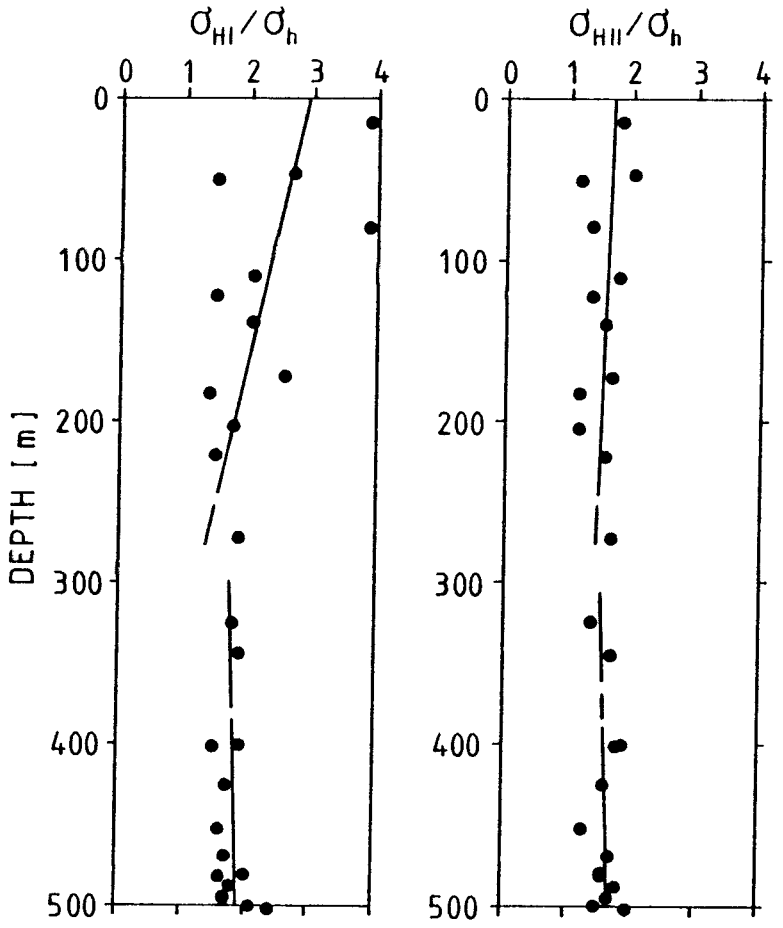

Figure 20. The ratio of maximum to minimum horizontal stresses versus depth for the first and the second breakdown methods. Linear regression of points above and below the discontinuity around 300 m depth.

5.4 Interpretation according to the first or the second brekdown method

In the majority of articles on hydrofracturing stress measurements the authors apply only one of the two possible evaluation methods for the maximum horizontal stress. This is often done without any comments or explanation.

The hydrofracturing measurements at Stripa (Doe et al. 1983) constitute one of the very few cases where both methods are applied and the results presented. The difference between the σ_H magnitudes from the two methods at Stripa is quite large, especially near the surface, the

second breakdown method giving the lower values. The authors reject the second breakdown method in the final evaluation of the state of stress because "the horizontal stress magnitudes, from overcoring and hydraulic fracturing, agree closely when the hydraulic fracturing data are interpreted using the first breakdown method", cit. Doe et al. 1983 p. 61.

On the other hand Hickman and Zoback (1983) prefer the second breakdown method stating that "due to the observed scale dependence of tensile strengths there can be considerable uncertainty in the extrapolation of laboratory-determined tensile strengths to in-situ conditions and, there can be considerable variation in the tensile strength of any rock unit within a given well", cit. Hickman and Zoback (1983) p. 51.

Applying the first breakdown method we assume that we have found a satisfactory method to extrapolate tensile strength data from 10 mm boreholes in the laboratory to the 56 mm hole in the field. Furthermore we assume a uniform tensile strength at all depths in the test hole. The first assumption is difficult to verify. For the second assumption we recall the results from the laboratory hydraulic fracturing tests on drillcores from Gi-1.

Depth (m)	T_{lab} (MPa)
50	12.6
150	19.4
250	17.9
380	18.3
460	22.3

All the samples are classified as migmatite gneiss. The tensile strength varies from 12.6 to 22.3 MPa. Each figure in the Table is a mean value from a series of tests. For individual specimens the variation is even larger. Figure 14 in Chapter 4 shows the tensile strength for individual specimens of two rock types in Gi-1, found from the Brazilian test. Again the variation in tensile strength is quite large. The assumption of a uniform tensile strength at all depths in Gi-1 is obviously not a good one.

The use of the second breakdown method rests on the assumption that no water penetrates the hydrofracture during pressurization in the second and subsequent cycles. According to theory the fracture is assumed to open up suddenly when the borehole pressure reaches the value of $3\sigma_h - \sigma_H$. The validity of this assumption depends on the rock type and the "quality" of the induced fracture, i.e. if it closes tightly at the borehole wall after depressurization. It also depends on the borehole pressurization rate.

Assume that a hydrofracture behaves ideally, not admitting any water at pressures lower than $3\sigma_h - \sigma_H$. What would we expect the pressure-time curve from a reopening test on this fracture to look like? For a constant pumping rate in all cycles the reopening curve should be a replica of the first pressurization cycle, up to the point of reopening, where it would deviate from the first one. The reopening curves from Gi-1 generally show a behaviour very close to the ideal one, with a linear pressure built-up parallel to the curve from the first cycle. The typical curve in Figure 3 shows these characteristics clearly.

The field tensile strength, ($T_f = P_{c1} - P_{c2}$), is an indirect measure of the rock quality. For borehole Gi-1 in Gideå it varies from 3 MPa to 14.7 MPa. The mean value of all 25 tests is 9.2 MPa. This is by far the highest T_f obtained from hydraulic fracturing stress measurements in Sweden so far.

Table 4. Mean values for T_f from hydraulic fracturing stress measurements in Sweden.

Site	$T_{f\ mean}$ (MPa)	Report
Stripa 1981	4.4	Doe et al. (1983)
Forsmark 1982	5.4	Stephansson and Ångman (1984)
Stidsvig 1983	1.8	Stephansson and Ångman (1984)
Bolmen 1985	5.5	Bjarnason et al. (1986)
Gideå 1985	9.2	This report

From the discussion above we find it justified to favour the second brekdown method in determining the maximum horizontal stress at Gideå.

5.5 Estimated error for the magnitudes of horizontal stresses

A rough estimate of the maximum error in determining the horizontal stress magnitudes from the pressure-time curves is given below.

If the instantaneous shut in pressure, P_s is taken as a direct measure of σ_h, the error in the minimum horizontal stress will be the same as the error in determining P_s. For good quality recordings, as those from Gideå, this error is estimated to lie within $\pm$ 5%.

The calculated maximum horizontal stress involves the term three times σ_h. Thus, any error in the determination of σ_h will be amplified in the calculation of σ_H. Furthermore, the second breakdown method involves the second breakdown pressure, P_{c2}. The determination of P_{c2} from the pressure-time curves is not as straight forward as it is for P_s. Where exactly does the second pressurization curve start to deviate from the first one? We find it satisfactory to set the error interval to $\pm$ 10% of the determined value. For the Gideå results the combined effect of these two sources of error will result in a final

error in σ_H ranging from 12.5 to 29 % for individual test sections, depending on the ratio between P_s and P_{c2} in each case. The mean error in σ_H for all 25 points is $\pm$ 18.2 %.

5.6 Stress orientations

Two, long and vertical hydrofractures were observed in 13 test sections. The mean strike of the two fractures in each test section is taken as the direction of the maximum horizontal stress at the corresponding depth. Most of the fracture directions fall within a sector of approximately 45^0, from N45^0E to E, see Figure 21 and Table A2 in the Appendix. Two outliers are noted at depths of 173 and 183 m. These two points are excluded from the evaluation. The mean value of the remaining eleven points in Figure 21 is N67^0E and this value is taken to represent the average orientation of the maximum horizontal stress in the test area. The orientation of the maximum horizontal stress with respect to the local fracture zones at the ground surface is shown in Figure 22.

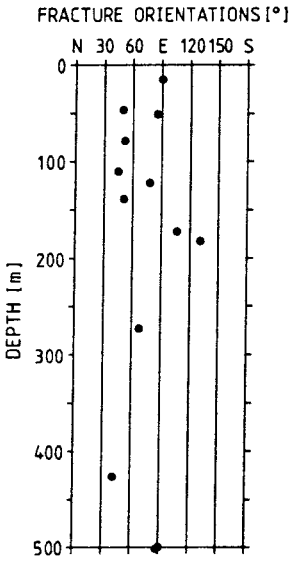

Figure 21. Hydrofracture orientations in borehole Gi-1 at Gideå.

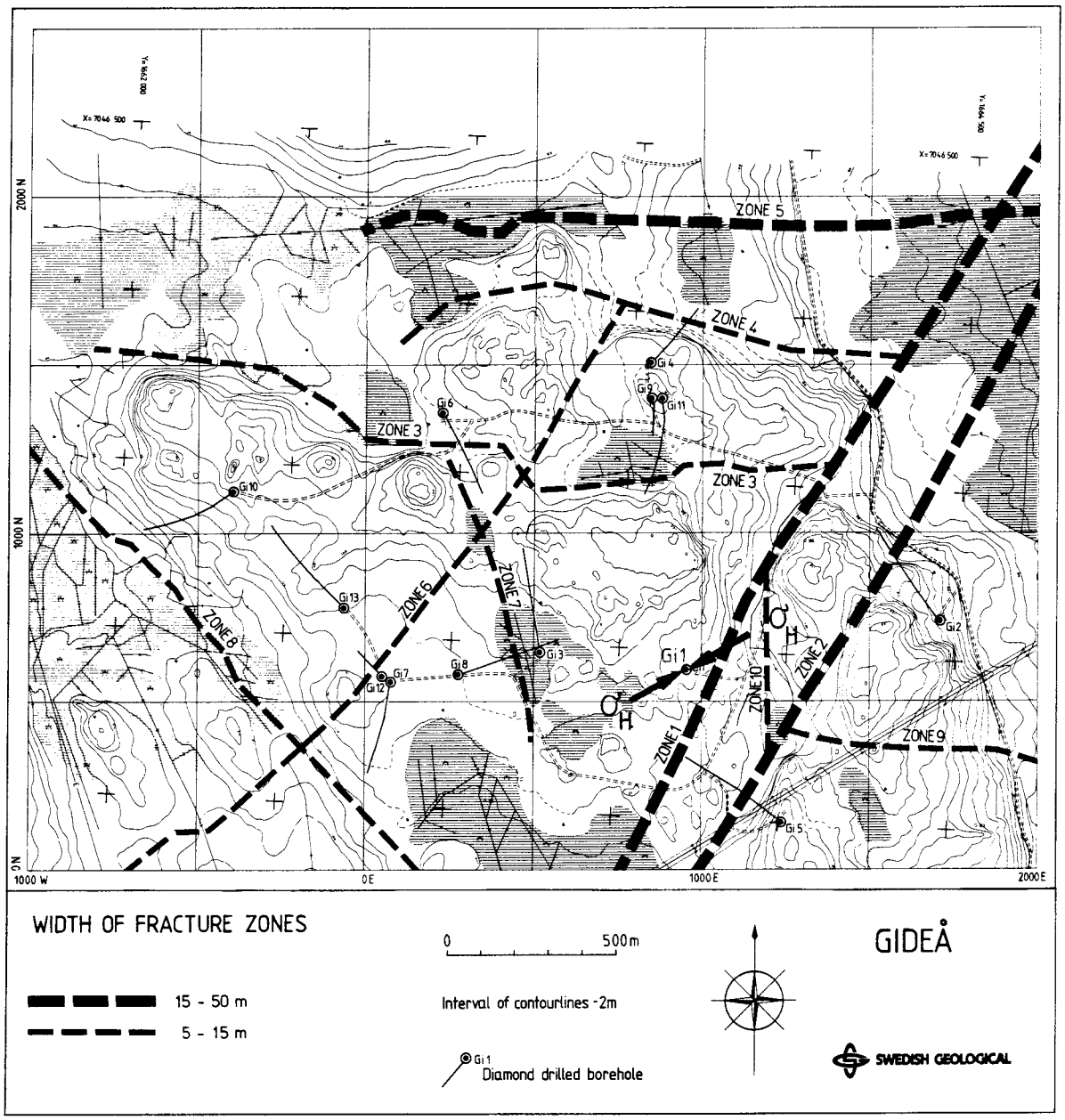

Figure 22. Orientation of the maximum horizontal stress with respect to the local fracture zones at surface.

The error inherent in the method used to determine the fracture orientations is estimated to be $\pm 10^0$. Keeping in mind the possible deviation of the induced fractures from the true orientaion of σ_H at each point due to rock anisotropy, and the natural variability of stress orientations within a rock mass it is obvious that this value is to be considered as a good estimate of the average orientation of σ_H.

6 CONCLUSIONS

6.1 The stress field

- The horizontal stress field at Gideå is moderate in magnitude, no extreme values have been recorded.

- The minimum horizontal stress increases continuously with depth, from 2 MPa close to the surface to roughly 11 MPa at 500 m depth. The scatter in the measured values is low. At approximately 300 m depth there is a change in the gradient of the minimum horizontal stress. Above that depth σ_h and the vertical stress increase at similar rates. Below 300 m the gradient is lower. The change in the gradient of σ_h coincides with reduced fracture frequency and hydraulic conductivity from 300 m depth in the rock mass in Gideå, and especially in the stress measurement borehole. As the difference in magnitude between σ_h and σ_v is generally small (<2 MPa), the stress field can be described as close to isotropic in the vertical plane containing σ_h and σ_v.

- The maximum horizontal stress is interpreted according to the second breakdown method, applying tensile strength values from the field measurements in the calculation of σ_H. At surface the value of σ_H is 2-3 MPa, increasing with depth at a higher rate than the minimum horizontal stress. At 500 m depth the maximum horizontal stress is around 19 MPa.

- The ratio between the maximum and the minimum horizontal stress, σ_H/σ_h, has a nearly constant value of 1.6 at all depths.

- The average orientation of the maximum horizontal stress is N67^{0}E. The orientation of σ_H does not tend to rotate with depth for the uppermost 500 m in the rock mass at Gideå.

6.2 Quality of the results

In general the results obtained from the stress measurements at Gideå are of good quality.

The pressurization rate during the fyrst cycle is constant, resulting in a straight line up to the point of breakdown. After breakdown the pressure in the test section falls steeply down to the instantaneous shut-in pressure. The post shut-in part of the curve is nearly linear and the pressure drop is very slow. During the second pressurization cycle the pressurization rate is constant again, resulting in a straight line parallel to the curve from the first cycle. At a pressure somewhat lower than the peak the curve deviates from the previous curve. The tensile strength of the rock in Gideå is generally high.

The reasons for the almost ideal shape of the curves are probably the following:

Test conditions:

- Rock stresses are moderate in the area. The hydrofracturing method works best at moderate to high rock stresses.

- The rock is brittle and has very low matrix permeability resulting in linear pressure built-up and sudden failure.

- Test sections free of fractures. The hydrofracture generally initiates and propagates in intact rock. Thus the post shut-in pressure does not bleed out through an existing fracture network.

Instrumentation:

- The pump- and water control system has been rebuilt and modified for exact flow rate control. Pressure surges have thus been eliminated and the pressure curves are smooth. This simplifies the evaluation process.

7 ACKNOWLEDGEMENTS

The authors are indebted to Mr Arne Torikka and Mr Kjell Bergström for their skilled and dedicated work on the development of the field instruments, and for their major contribution to the field work at Gideå.

8 REFERENCES

Ahlbom, K., Albino, B., Carlsson, L., Nilsson, G., Olsson, O., Stenberg, L. and Timje, H. (1983). Evaluation of the geological, hydrogeological and geophysical conditions at Gideå. SKB/KBS Technical Report 83-53. Swedish Nuclear Fuel and Waste Management Co., Stockholm.

Bjarnason, B., Leijon, B. and Stephansson, O. (1986). The Bolmen Project. Rock Stress Measurements Using Hydraulic Fracturing and Overcoring Techniques. BeFo (Swedish Rock Engineering Research Foundation, Stockholm) report series (in press)

Doe, T.W., Ingevald, K., Strindell, L., Leijon, B., Hustrulid, E., Majer, E. and Carlsson, H. (1983). In Situ Stress Measurements at the Stripa Mine, Sweden. Report LBL-15009, SAC44. Swedish-American Cooperative Program on Radioactive Waste Storage in Mined Caverns in Crystalline Rock. 251 p.

Haimson, B.C. (1978). The Hydrofracturing Stress Measuring Method and Recent Field Results. Int. J. Rock Mech. Min. Sci. & Geomech. Abstr., 15, pp. 167-178.

Hickman, S. and Zoback, M.D. (1983). The Interpretation of Hydraulic Fracturing Pressure-Time Data For In-Situ Stress Determination. Proc. Workshop Hydraulic Fracturing Stress Measurements. U.S. National Committee for Rock Mechanics, Washington, D.C., pp. 44-54.

Hubbert, M.K. and Willis, D.G. (1957). Mechanics of Hydraulic Fracturing. Trans. A.I.M.E., 210, pp. 153-168.

Ljunggren, C., Stephansson, O., Alm. O., Hakami, H. and Mattila, U. (1985). Mechanical properties of granitic rocks from Gideå, Sweden. SKB Technical Report 85-06. Swedish Nuclear Fuel and Waste Management Co., Stockholm.

Paris, P. and Sih, G. (1965). Stress Analysis of a Crack. In: Fracture Toughness and its Testing. American Society of Testing and Materials Special Publications, Baltimore, 381, pp. 30-83.

Rummel, F., Baumgärtner, J. and Alheid, H.J. (1983). Hydraulic Fracturing Stress Measurements Along the Eastern Boundary of the SW-German Block. Proc. of a Workshop on Hydraulic Fracturing Stress Measurements, Dec. 2-5, 1981, Nationla Academic Press, Washington, D.C. pages 3-17.

SKBF/KBS (1983). Final Storage of Spent Nuclear Fuel - KBS-3. Part IV Safety. Swedish Nuclear Fuel and Waste Management Co., Stockholm.

Stephansson, O. and Ångman, P. (1986). Hydraulic fracturing stress measurements at Forsmark and Stidsvig, Sweden. Bull. Geol. Soc., Finland 58, Part 1. (in press)

Zoback, M.D. and Haimson, B.C. (1982). Status of the Hydraulic Fracturing Method for In-Situ Stress Measurements. Issues in Rock Mechanics Proc. 23rd U.S. Symp. on Rock Mech., Univ. of California, Berkeley, Cal., August 25-27, pp. 143-156.

Ångman, Per (1984). Bergspänningsmätning med hydraulisk spräckning i Stidsvig, Skåne. Graduate thesis 1984:035 E, Luleå University of Technology, Sweden. 57 p. (in Swedish)

APPENDIX

Table A1. Pressure data from borehole Gi-1.

Depth	P_{c1}	P_{c2}	P_{c3}	P_{c4}	P_{s1}	P_{s2}	P_{s3}	P_{s4}
14.5	9.4	2.7	2.7	2.6	2.3	2.2	1.9	1.5
47.0	12.0	1.8	1.7	1.5	1.8	1.8	1.5	1.1
51.0	14.6	3.7	3.7	3.8	2.1	2.0	2.1	2.1
79.5	8.3	5.3	4.7	4.6	3.6	3.8	3.2	3.2
111.0	15.4	5.1	4.8	4.5	4.3	4.4	4.4	4.3
122.5	19.1	8.1	8.1	8.1	5.6	5.3	5.2	5.0
140.0	17.3	9.5	9.4	9.1	7.1	7.1	6.4	6.2
173.0	13.5	6.8	6.6	6.2	5.8	5.5	5.3	5.2
183.0	24.5	14.6	14.1	13.1	8.9	8.5	8.0	7.9
204.0	20.1	13.3	13.2	12.5	7.6	7.2	7.3	7.2
222.0	22.3	10.5	10.3	10.0	7.8	7.4	7.4	7.5
273.0	21.4	11.2	11.2	11.0	9.1	8.6	8.7	9.1
325.0	21.7	14.0	13.6	13.4		8.6	8.9	8.8
345.0	23.8	14.5	14.5	14.2	11.5	10.9	11.2	11.1
400.9	23.7	12.8	12.7	12.0	11.8	11.1	11.5	11.7
402.0	28.2	13.5	13.5	13.3	11.3	10.8	10.9	11.0
426.0	24.5	13.9	13.9	14.1	9.6	9.7	9.9	10.0
453.0	25.6	17.6	17.7	17.5	10.2	10.2	10.1	9.9
470.0	26.9	15.2	15.2	14.9	12.1	11.4	11.7	12.0
481.5	23.6	17.1	17.0	16.2	13.2	12.7	12.5	12.7
483.0	28.5	17.0	17.0	16.7	12.8	11.9	12.1	12.2
489.0	25.7	14.3	13.4	13.5	11.9	11.7	12.1	12.2
495.0	25.5	14.6	14.3	13.8	11.9	10.9	11.3	10.9
500.0	20.6	15.1	15.0	14.2	10.5	10.3	10.2	10.4
501.0	16.9	10.1	10.0	9.3	10.0	9.8	10.0	10.1

All pressures in MPa

Table A2. Fracture orientations.

Depth (m)	$F1^0$	$F2^0$	$F2^0-F1^0$	F^0	Comments
14.5	90	271	181	90	+
47	49	231	182	50	+
51	60	291	231	85	+
79.5	66	219	153	52	+
100					S
111	44	225	181	45	+
122.5	85	251	166	78	+
140	64	217	153	51	+
173	104	290	186	107	+
183	131	314	183	132	+
204	167	324	157	156	(+)
222					0
245					S
273	65	250	185	68	+
303					S
325					0
339.4					S
345					U
363					S
382					S
400.9					0
402		195		15	(+)
426	45	218	173	42	+
453					U
470					U
481.5					0
483	111	302	191	116	(+)
489					0
495					0
500	87	272	185	90	+
501	84	270	186	87	+

$F1^0$, $F2^0$ = The orientation of each fracture measured clockwise from zero at N (360^0 circle). F^0 = The mean value of $F1^0$ and $F2^0$, $F^0 = (F1^0 + (F2^0-180^0))/2$. 0 = Old fractures of varying orientations. S = Subhorizontal fractures. U = Unsuccessful impression. + = Two vertical or near vertical hydrofractures. (+) = Vertical fractures of uncertain origin.

Table A3. Results from laboratory tests on core samples.

Depth (m)	σ_z (MPa)	P_c (MPa)	P_{ic} (MPa)
51.0	5.9	0	23.3
51.1	5.9	0	22.8
51.2	15.4	9.8	30.0
51.4	24.1	14.3	43.5
51.1	29.0	19.9	48.4
51.8	10.2	5.0	26.3
148.0	5.2	0	19.7
148.9	8.6	2.3	25.0
149.0	10.5	4.8	23.4
149.1	15.6	9.7	25.2
149.2	19.2	13.9	38.8
149.5	17.5	12.3	35.6
251.9	15.3	0	17.4
252.0	29.0	9.4	28.9
252.1	9.9	4.8	22.8
252.3	24.1	14.3	35.3

Depth (m)	σ_z (MPa)	P_c (MPa)	P_{ic} (MPa)
252.4	6.0	2.2	21.1
252.6	42.5	9.1	26.5
252.8	15.0	7.0	28.2
252.9	19.2	11.3	30.0
381.7	10.2	4.8	22.8
381.9	20.0	15.0	34.9
382.0	27.8	19.8	40.3
382.1	15.4	9.8	30.9
460.5	7.6	2.4	25.5
460.7	21.7	16.7	40.5
460.9	10.3	4.8	29.9
461.0	14.8	9.5	34.9
461.2	20.3	14.4	39.2
461.3	27.1	19.8	45.0
461.6	6.3	0	19.8

Regression lines:

Depth

50 m : $P_{ic} = 12.61 + 1.32\ P_c$ (MPa) $\quad r = 0.967$

150 m : $P_{ic} = 19.39 + 1.19\ P_c$ (MPa) $\quad r = 0.897$

250 m : $P_{ic} = 17.87 + 1.16\ P_c$ (MPa) $\quad r = 0.974$

380 m : $P_{ic} = 18.33 + 1.13\ P_c$ (MPa) $\quad r = 0.989$

460 m : $P_{ic} = 22.31 + 1.16\ P_c$ (MPa) $\quad r = 0.984$

PRESSURE-TIME CURVES FROM THE FIELD MEASUREMENTS

Explanations to the test curves are shown on Figure 3 in chapter 2.

Full scale (100) on the vertical axis = 50 MPa

14.5 m

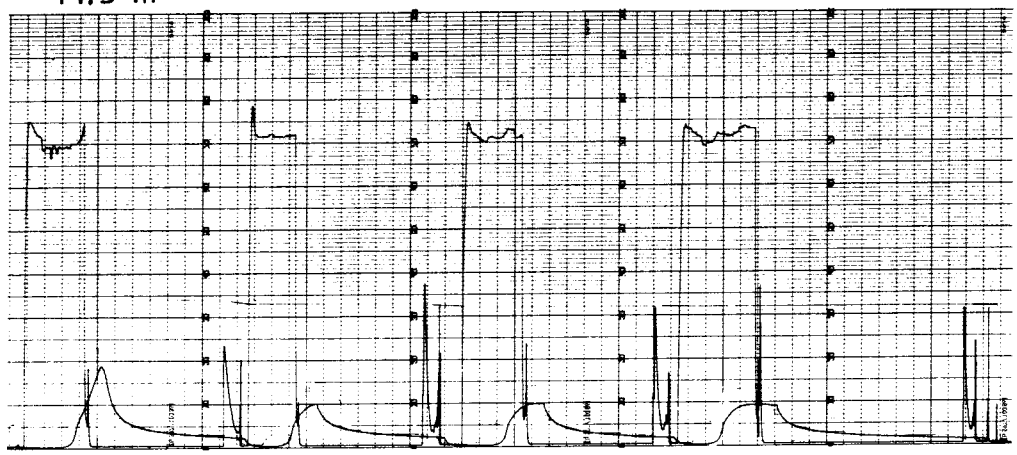

47 m

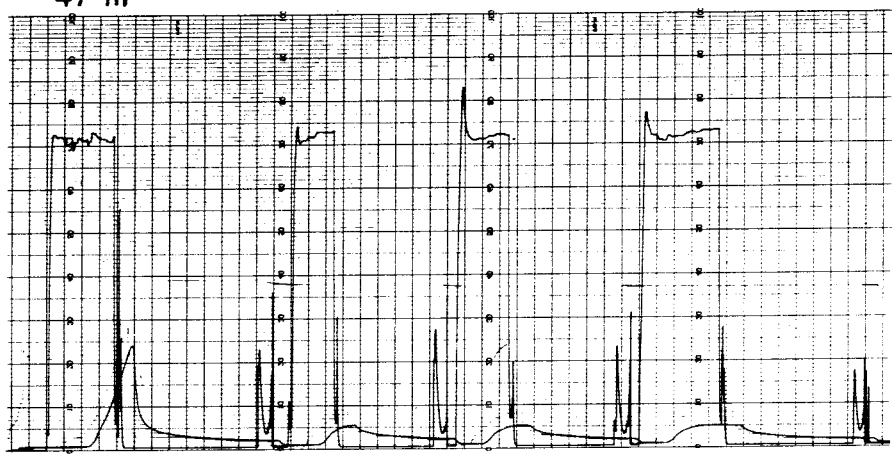

51 m

111 m

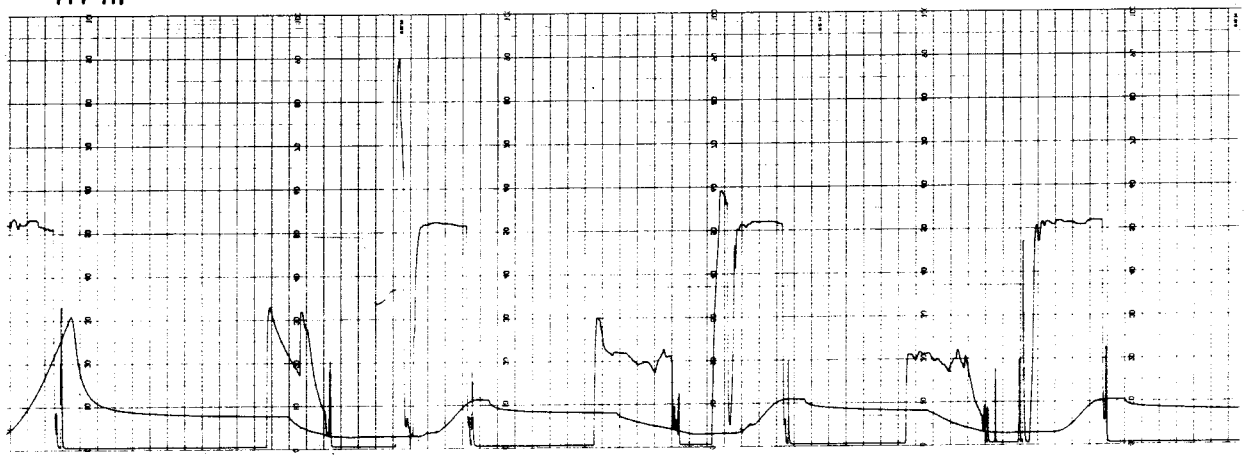

140 m

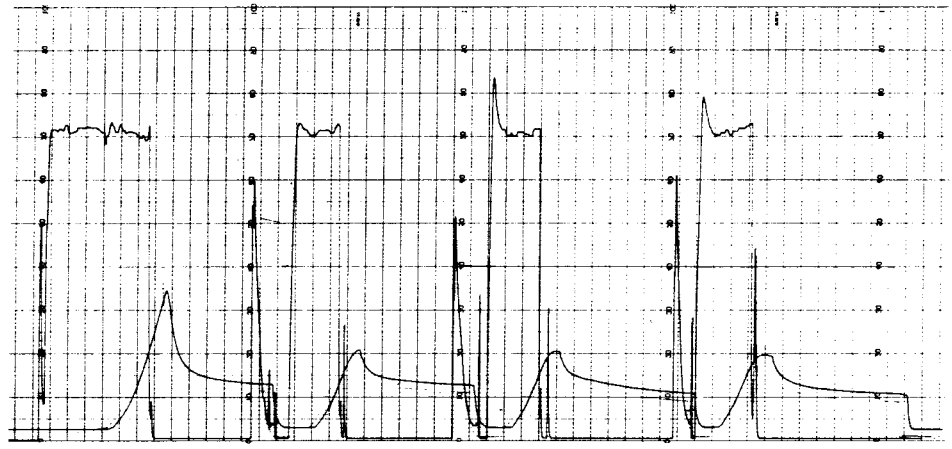

183 m

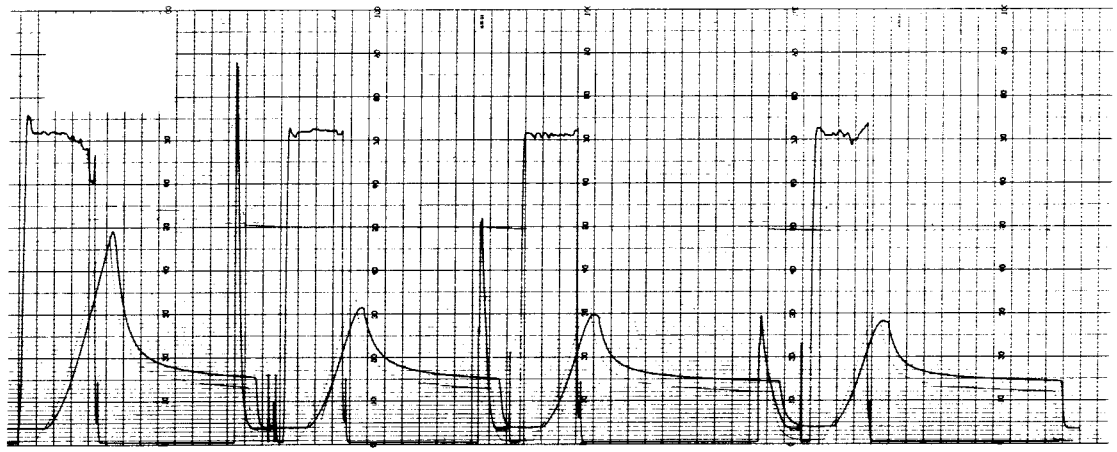

204 m

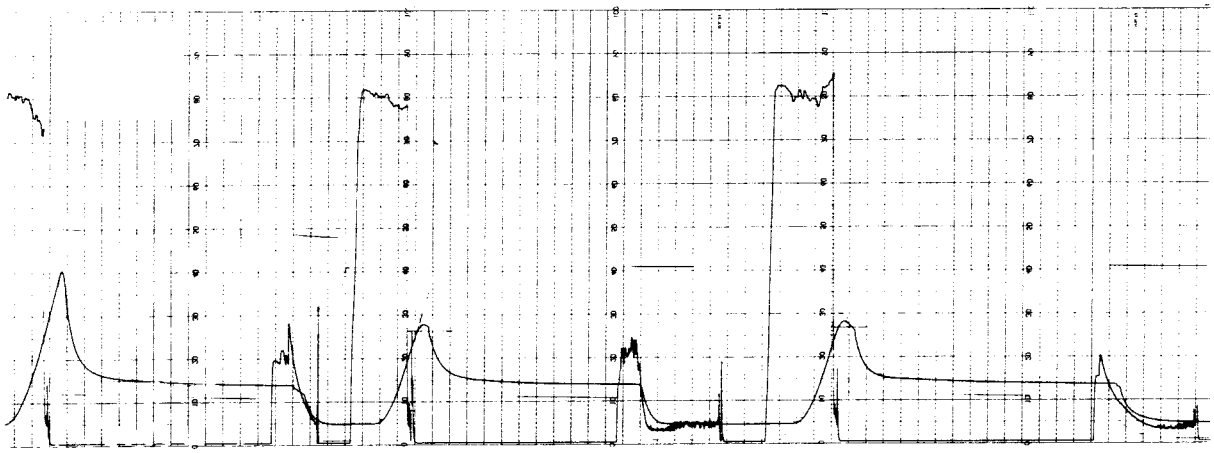

273 m

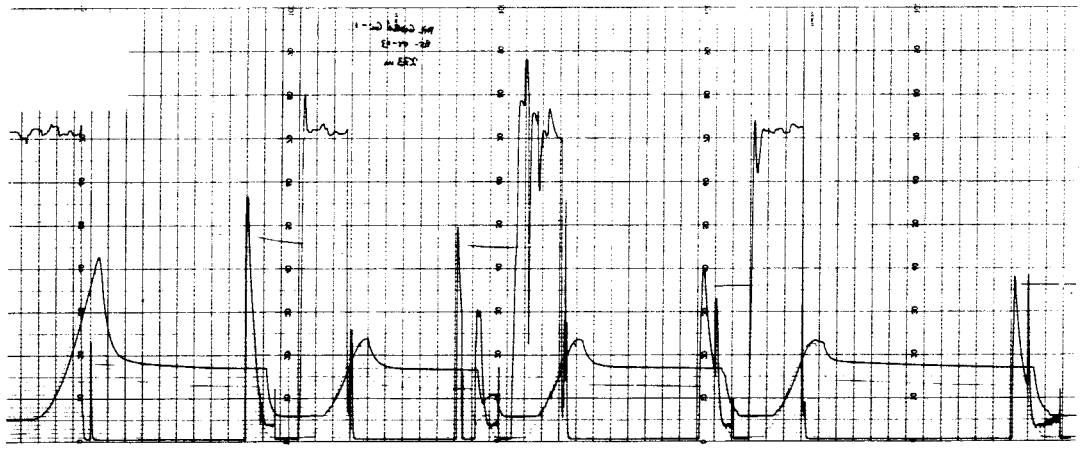

345 m

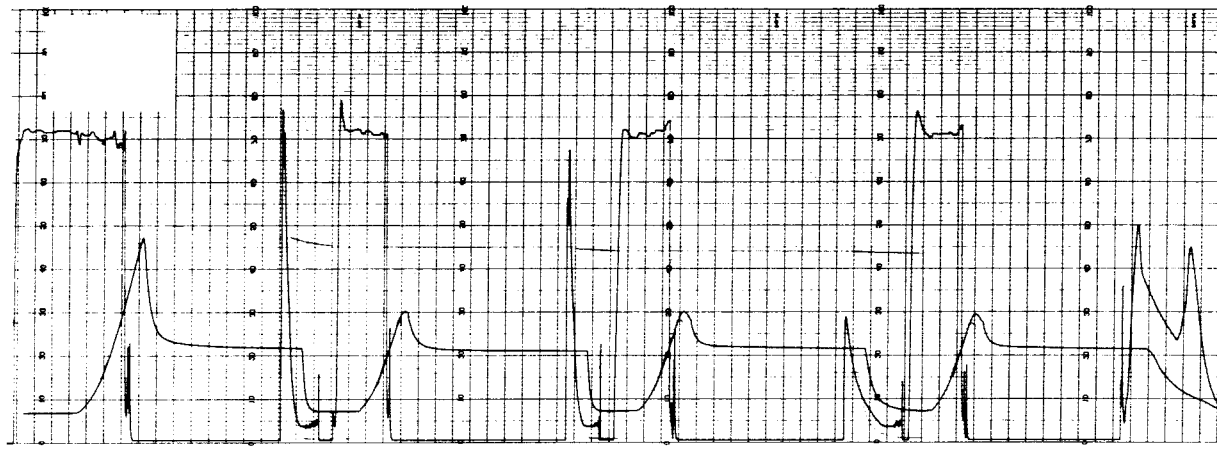

400.9 m

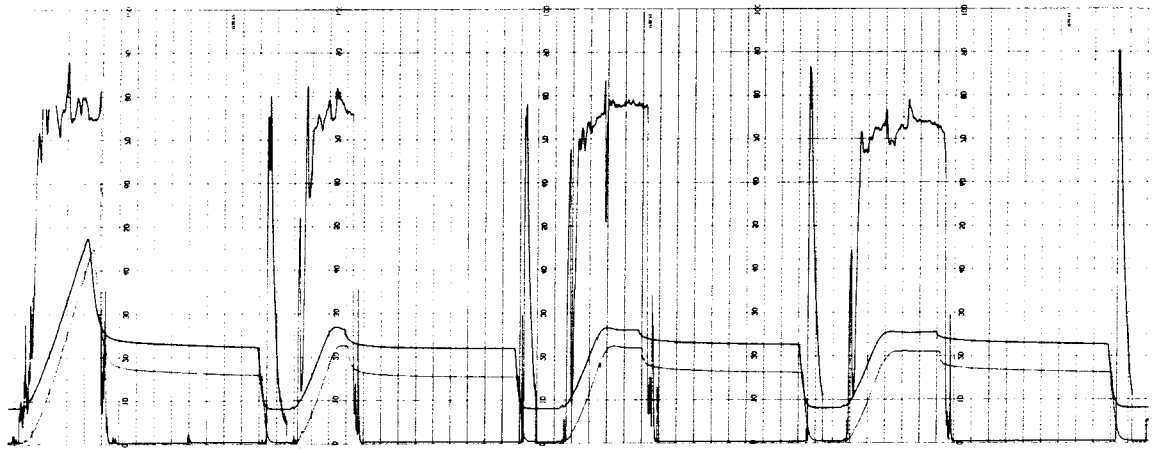

426 m

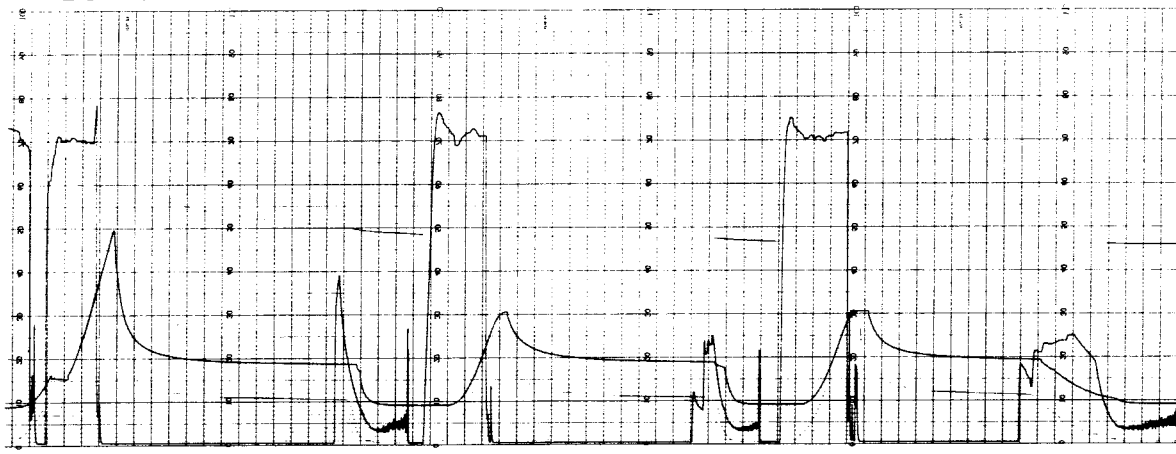

453 m

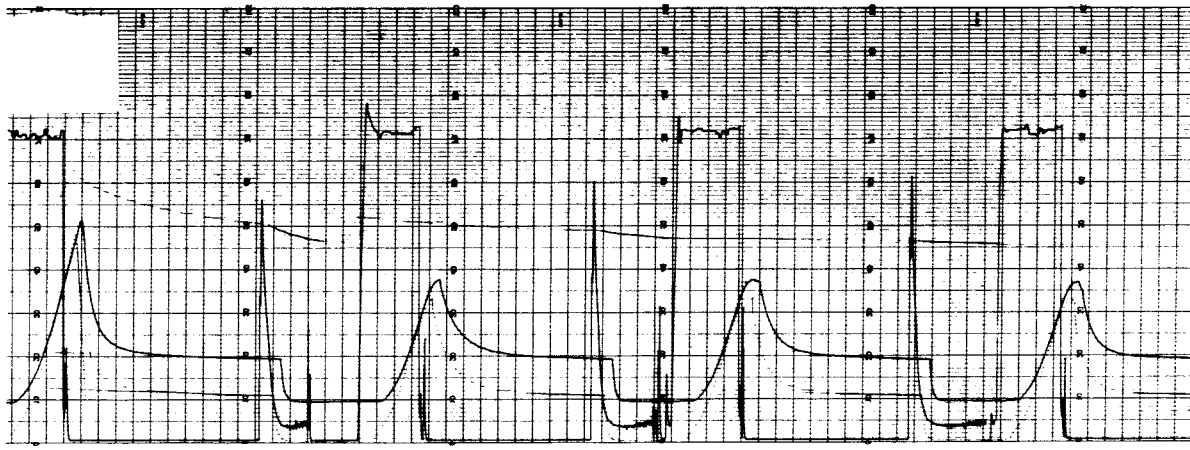

470 m

481.5 m

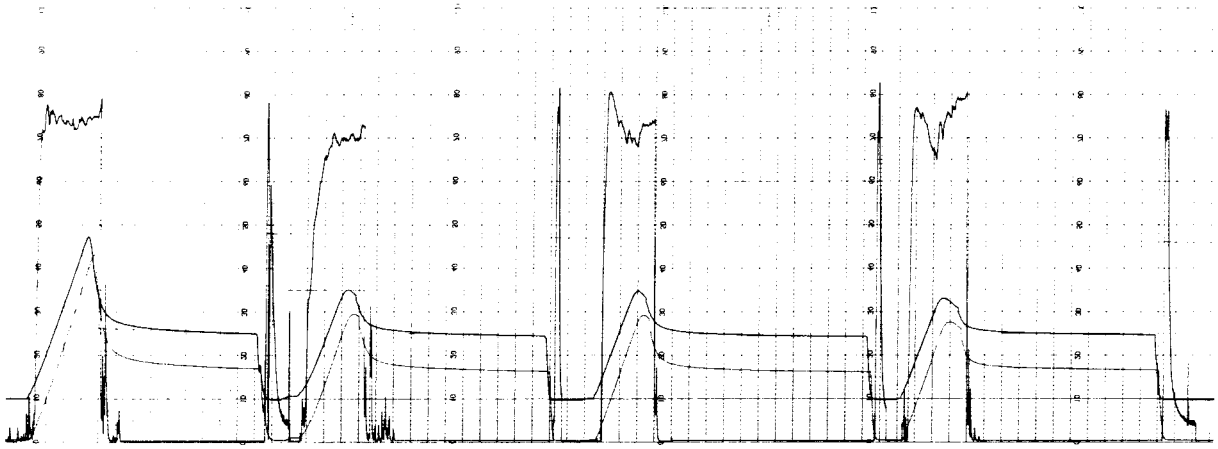

483 m

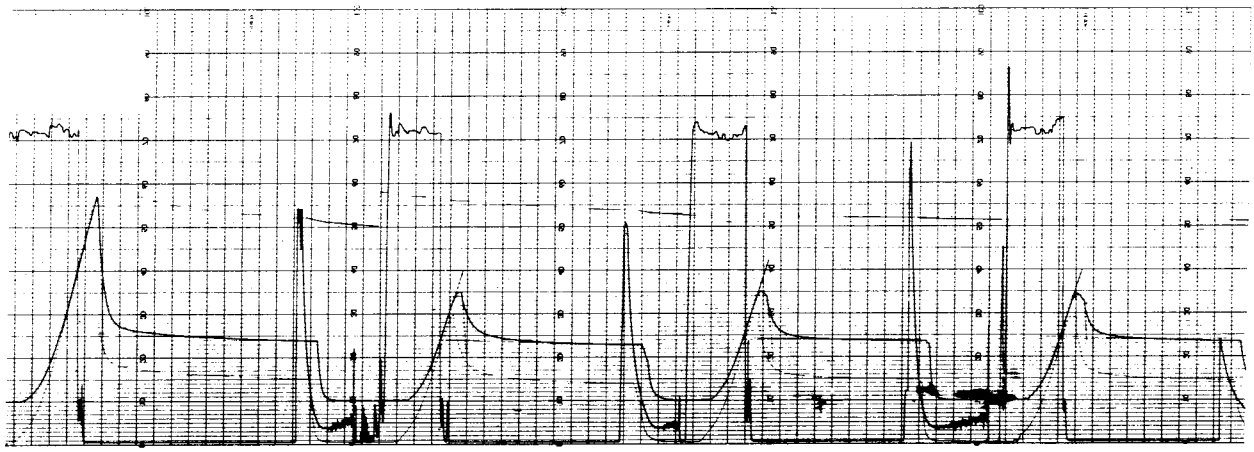

489 m

495 m

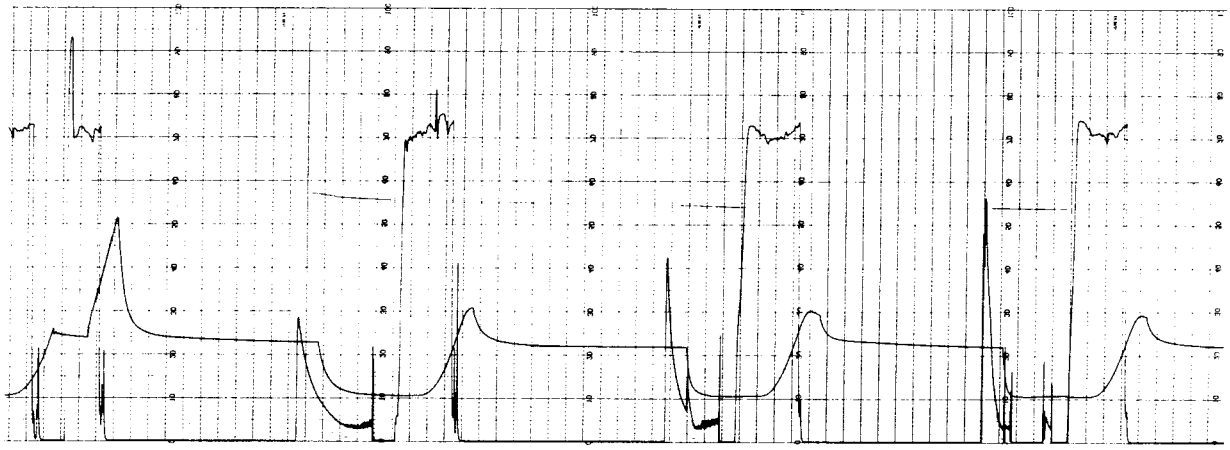

500 m

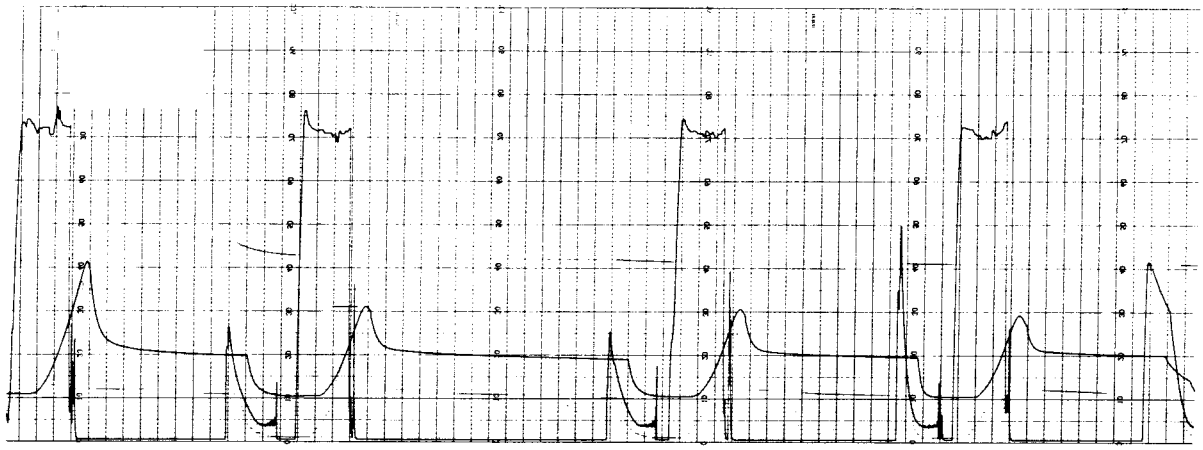

501 m

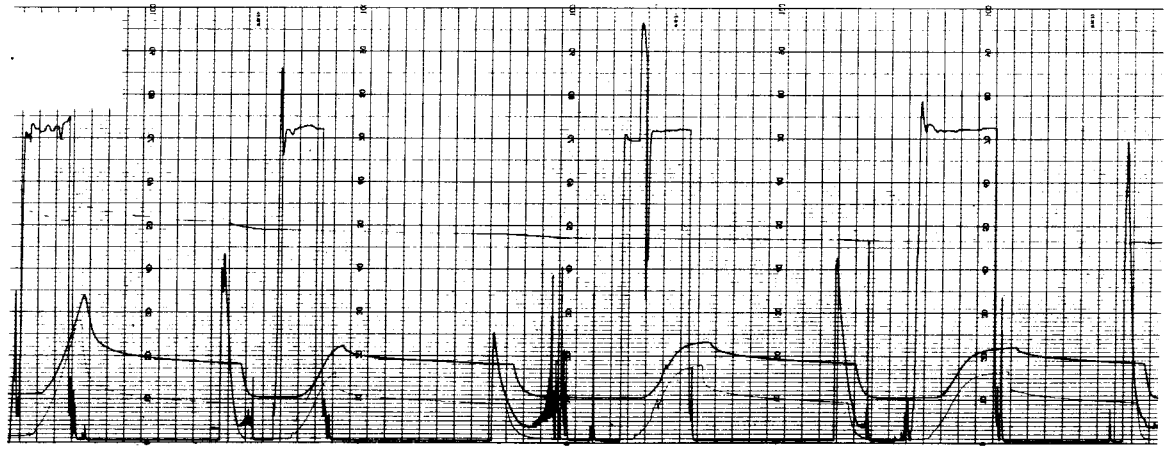

List of SKB reports

Annual Reports

1977–78
TR 121
KBS Technical Reports 1 – 120.
Summaries. Stockholm, May 1979.

1979
TR 79–28
The KBS Annual Report 1979.
KBS Technical Reports 79-01 – 79-27.
Summaries. Stockholm, March 1980.

1980
TR 80–26
The KBS Annual Report 1980.
KBS Technical Reports 80-01 – 80-25.
Summaries. Stockholm, March 1981.

1981
TR 81–17
The KBS Annual Report 1981.
KBS Technical Reports 81-01 – 81-16.
Summaries. Stockholm, April 1982.

1982
TR 82–28
The KBS Annual Report 1982.
KBS Technical Reports 82-01 – 82-27.
Summaries. Stockholm, July 1983.

1983
TR 83–77
The KBS Annual Report 1983.
KBS Technical Reports 83-01 – 83-76
Summaries. Stockholm, June 1984.

1984
TR 85–01
Annual Research and Development Report 1984
Including Summaries of Technical Reports Issued during 1984. (Technical Reports 84-01– 84-19)
Stockholm June 1985.

1985
TR 85-20
Annual Research and Development Report 1985
Including Summaries of Technical Reports Issued during 1985. (Technical Reports 85-01-85-19)
Stockholm May 1986.

Technical Reports

1986

TR 86-01
I: An analogue validation study of natural radionuclide migration in crystalline rock using uranium-series disequilibrium studies
II: A comparison of neutron activation and alpha spectroscopy analyses of thorium in crystalline rocks
J A T Smellie, Swedish Geological Co, A B MacKenzie and R D Scott, Scottish Universities Research Reactor Centre
February 1986

TR 86-02
Formation and transport of americium pseudocolloids in aqueous systems
U Olofsson
Chalmers University of Technology, Gothenburg, Sweden
B Allard
University of Linköping, Sweden
March 26, 1986

TR 86-03
Redox chemistry of deep groundwaters in Sweden
D Kirk Nordstrom
US Geological Survey, Menlo Park, USA
Ignasi Puigdomenech
Royal Institute of Technology, Stockholm, Sweden
April 1, 1986

TR 86-04
Hydrogen production in alpha-irradiated bentonite
Trygve Eriksen
Royal Institute of Technology, Stockholm, Sweden
Hilbert Christensen
Studsvik Energiteknik AB, Nyköping, Sweden
Erling Bjergbakke
Risö National Laboratory, Roskilde, Denmark
March 1986

TR 86-05
Preliminary investigations of fracture zones in the Brändan area, Finnsjön study site
Kaj Ahlbom, Peter Andersson, Lennart Ekman, Erik Gustafsson, John Smellie,
Swedish Geological Co, Uppsala
Eva-Lena Tullborg, Swedish Geological Co, Göteborg
February 1986

TR 86-06
Geological and tectonical description of the Klipperås study site
Andrzej Olkiewicz
Vladislav Stejskal
Swedish Geological Company
Uppsala, June 1986

TR 86-07
Geophysical investigations at the Klipperås study site
Stefan Sehlstedt
Leif Stenberg
Swedish Geological Company
Luleå, July 1986

TR 86-08
Hydrogeological investigations at the Klipperås study site
Bengt Gentzschein
Swedish Geological Company
Uppsala, June 1986

TR 86-09
Geophysical laboratory investigations on core samples from the Klipperås study site
Leif Stenberg
Swedish Geological Company
Luleå, July 1986

TR 86-10
Fissure fillings from the Klipperås study site
Eva-Lena Tullborg
Swedish Geological Company
Göteborg, June 1986